The right visual field advantage in crowding is specific to letters

Alex White*, Nicole Oppenheimer & Anishka Yerabothu

Department of Neuroscience & Behavior
Barnard College, Columbia University
3009 Broadway
New York, NY, 10027
USA

*Corresponding author. Email: alwhite@barnard.edu

Abstract

Visual crowding is the impairment to object recognition caused by similar objects that are too close to the target. Although crowding occurs in many contexts, it is not clear whether the underlying mechanisms are the same for all stimulus categories. One clue is that crowding is sometimes less severe in the right visual hemifield than in the left. However, this hemifield asymmetry has emerged most often in letter identification tasks. Here we investigated whether the hemifield asymmetry is a general attribute of crowding or specific to identifying familiar letters. In three experiments, we precisely measured *crowding distances* (the spacing between targets and flankers required to reach a threshold level of accuracy) in each hemifield for several types of stimuli: Latin letters, pseudo-letters with matched visual features, Landolt squares, and face icons. For letters only, crowding distances were significantly smaller in the right visual field than in the left. This asymmetry was larger for letters than for all other stimulus types. The asymmetry for letters persisted even when the target letter was flanked by unfamiliar pseudo-letters, demonstrating that it is not simply an advantage for processing strings of letters. Two other findings support stimulus-specific mechanisms: the patterns of flanker substitution errors and across-participant correlations in crowding distances. We propose that reading experience strengthens connections between left-hemisphere language areas and left-hemisphere visual cortex, leading to specific letter-processing mechanisms with more precise spatial tuning in the right visual hemifield.

Keywords: crowding; object recognition; letter recognition; lateralization; hemifield asymmetry; reading

Introduction

Crowding

Objects are easier to recognize at the center of gaze than in the peripheral visual field. This simple fact is caused by several factors in the physiology of the visual system, which are not completely understood. For instance, the density of photoreceptors varies across the retina, which helps account for differences in *acuity*. Acuity determines the smallest shape (such as a letter) that you can identify when it is presented alone on an uncluttered background. Acuity worsens with increasing eccentricity (distance from fixation).

But acuity is only part of the story (Song et al., 2014; Strasburger, 2020). Your ability to identify objects is also affected by *crowding*: a single object might be easily identifiable when presented alone, but it becomes unrecognizable if similar shapes are close to it (Bouma, 1970; Ehlers, 1936, 1953; Mackworth, 1965). Crowding is this interference to recognition caused by flanking objects.

Crowding is thought to be a general property of object recognition (Pelli & Tillman, 2008). It impairs perception of many categories of stimuli, from simple lines and gratings, moving patterns, and colors, to faces and common objects (Greenwood et al., 2017; Greenwood & Parsons, 2020; Herzog & Manassi, 2015; Manassi & Whitney, 2018; Martelli et al., 2005; Pelli & Tillman, 2008; Wallace & Tjan, 2011; Whitney & Levi, 2011).

It would therefore be parsimonious to explain crowding by a single mechanism that arises at a relatively early stage of visual processing and affects all types of stimuli. For example, some models state that crowding is caused by obligatory "pooling" of the features of targets and flankers within inappropriately large "integration zones" (Parkes et al., 2001; Pelli et al., 2004; Rosenholtz et al., 2019). Alternatively, other models allow for crowding to occur at multiple stages of the visual hierarchy (Manassi & Whitney, 2018), with perceptual judgments being determined by sampling from neurons that are tuned to the target's category (Chaney et al., 2014). Thus, some researchers propose different underlying mechanisms of crowding for specific stimulus categories, such as letters (Grainger et al., 2010), although this is debated (Castet et al., 2017).

Mechanistic models must also account for how crowding differs across the visual field. Like acuity, crowding worsens with increasing eccentricity. Specifically, the *crowding distance* increases with eccentricity (Bouma, 1970; Kurzawski et al., 2023; Toet & Levi, 1992). The crowding distance is the minimum distance between the center of the target and the center(s) of the flanker(s) that is required for an observer to identify the target with a threshold level of accuracy.

In addition to varying with eccentricity, crowding also differs *around* the visual field: it is stronger along the vertical than horizontal meridian, and stronger above than below fixation. These two asymmetries are consistent across several stimulus types (including letters and simple shapes; Kurzawski et al., 2023) and they mirror similar asymmetries observed for measures of contrast sensitivity and acuity (Himmelberg et al., 2023).

The hemifield asymmetry for crowding

A third asymmetry has emerged in some studies of crowding, but not all: a *hemifield* asymmetry, due to weaker crowding in the right visual field than the left. Early studies noted that participants are better able to report crowded *letters* that are flashed in the right visual field than in the left (Bouma, 1973; Crovitz & Schiffman, 1965). Bouma (1973) described the crowding phenomenon as "visual interference of a masking type," which operates outwards in, meaning that a target is most crowded by a flanker positioned farther into the periphery than it is. To explain the right visual field advantage, Bouma proposed that "the spatial extent of foveally oriented masking" is smaller in the right visual field than the left. The right visual field advantage for crowded letters has been found in several subsequent studies (Callens et al., 2013; Estes et al., 1976; Grainger et al., 2010; Huckauf & Heller, 2002; Kurzawski et al., 2023; Ramamurthy et al., 2021; Shechter et al., 2024; Winsler & Luck, 2025).

Crowding and its hemifield asymmetry have important implications for reading. A closely related concept is the *visual span*: a measure of how far out to either side of fixation letters in short strings can be identified (Legge et al., 2001, 2007). The visual span extends farther to the right of fixation than the left, likely due to weaker crowding in the right visual field. Pelli et al. (2007) describe the visual span as the "uncrowded window" through which we can read. This framing suggests readers with smaller crowding distances could process more text during each gaze fixation. Consistent with that prediction, various measures of crowding correlate with literacy skills and are elevated in many individuals with dyslexia (e.g., Bertoni et al., 2019; Frömer et al., 2015; Gori & Facoetti, 2015; Joo et al., 2018; Liu et al., 2017; Martelli et al., 2009; Winsler & Luck, 2025).

This hemifield asymmetry for crowded letters relates to a hemifield asymmetry for whole word recognition. Single words are judged more accurately when they are flashed in the right visual field than in the left (Mishkin & Forgays, 1952). This finding has generated much interest in brain development and the lateralization of cognitive functions to cerebral hemispheres (Behrmann & Plaut, 2020; Brederoo et al., 2019; Dundas et al., 2013; Ossowski & Behrmann, 2015; A. L. White et al., 2019; M. J. White, 1969; Yeatman & White, 2021). For instance, is the right visual field advantage culturally universal, or is it specific to languages that are read from left to right? The evidence is somewhat mixed, but several studies have demonstrated a right visual field advantage for words in languages that are read leftwards,

including Arabic and Hebrew (Adamson & Hellige, 2006; Barton et al., 1965; Faust et al., 1993; Ibrahim & Eviatar, 2009, 2012; Siéroff & Haehnel-Benoliel, 2015). The hemifield asymmetry for crowded *letters* (smaller crowding distances on the right) is also present in Hebrew (Shechter et al., 2024).

Thus, the asymmetry of crowding for letters and the asymmetry of word recognition may have the same cause. But is that cause a domain-general property of vision, or is it specific to processing linguistic stimuli?

Is the hemifield asymmetry specific to crowded letters?

Kurzawski et al. (2023) reviewed several crowding studies and noted that the right-vs.-left hemifield asymmetry varies across categories of stimuli. All studies that used letter identification tasks demonstrate a strong asymmetry. One study reported no significant asymmetry for simple "tumbling clock" stimuli: circles containing a single line that participants judged the orientation of (Greenwood et al., 2017).

Only a small number of studies have directly compared the hemifield asymmetry for letters against other types of stimuli. One compared crowding distances for letters vs. other orthographic symbols (e.g., Σ, <, &,@,£, ∞) and reported a general right visual field advantage with no significant interaction between hemifield and stimulus type (Grainger et al., 2010). A more recent study came to a similar conclusion by comparing crowding distances for letters, inverted letters, and Gabor patches (Winsler & Luck, 2025). Although crowding distances were lowest for upright letters, the right visual field advantage did not significantly differ across stimulus types. However, Chanceaux et al. (2013) reported that accuracy was overall higher for crowded letters in the right visual field, but the *opposite* asymmetry emerged for simple outline shapes (squares, triangles, etc.). Thus, to date we have sparse and inconsistent evidence regarding the generality of the right visual field advantage in crowding.

This question has theoretical implications for mechanistic models of crowding. If the hemifield asymmetry is specific to one category of stimulus, then models that assume a single stage of feature integration might need to be revised. Models that assume crowding occurs in neurons tuned for a particular stimulus category would be less challenged. Both classes of models would need to explain how reading experience or cerebral lateralization affect crowding distances.

Outline of the present study

We conducted three experiments to examine the specificity of the hemifield asymmetry in crowding. We measure crowding distance thresholds in the right and left visual fields for four different stimulus types. All of the stimuli were composed of black lines on a white

background and can be directly compared in terms of size and spacing. On each trial, we presented a horizontally aligned set of three shapes, the center of which was the target to be identified. The task-irrelevant flankers were arranged *radially* relative to the point of gaze fixation (along the horizontal meridian in this case), which causes stronger crowding than tangentially aligned flankers (Kurzawski et al., 2023; Toet & Levi, 1992).

There are two competing hypotheses. On the one hand, if the hemifield asymmetry is a general property of crowding, then the right:left ratio of crowding distances should not significantly differ across types of stimuli. On the other hand, if the hemifield asymmetry is specific to legible orthographic stimuli, then only letters should have a right:left ratio significantly less than 1.

In Experiment 1, we compare crowding for trigrams of letters, "boxes" (Landolt squares with a gap on one side), and "emojis," face icons that differ in emotional expression. The letters never formed English words. We included the emojis due to prior evidence that while letters and words have a right visual field advantage, face perception has a left visual field advantage, at least in uncrowded conditions (Brederoo et al., 2019; Dundas et al., 2013; Hines, 1978; Leehey & Cahn, 1979).

In Experiment 2, we repeated the experiment but replaced the emojis with novel pseudo-letters that were constructed to match the Latin letters in terms of several visual features: size, symmetry, and number of strokes, junctions, and terminations (Vidal et al., 2017). We also randomly intermixed the three stimulus types so that differences in crowding could not be attributed to differences in attention.

In Experiment 3, we compared crowding for target letters flanked either by other letters or by pseudo-letters. This comparison allowed us to test whether the right visual field advantage for crowded letters is due to efficient processing of entire *strings* of legible letters. If so, then the asymmetry should disappear when a letter is flanked by non-letters.

In all three experiments, we fit full psychometric functions to characterize how accuracy varies with target-flanker spacing. Other recent studies that addressed the hemifield asymmetry estimated crowding distances with rapid staircase procedures (Kurzawski et al., 2023; Winsler & Luck, 2025). This approach allows for efficient testing of a large number of participants but requires assuming the slope and upper asymptote of the psychometric function. We fit those parameters to the data, in case stimulus types or hemifields differ in slope, or in how likely participants are to make an error even when the target-flanker spacing is large. This required collecting large numbers of trials per participant over multiple testing sessions.

To further probe how crowding differs across stimulus types, we also analyzed error patterns: how likely participants were to incorrectly report either the inner or outer flanker instead of the target (mislocalization or substitution errors; Freeman et al., 2012; Shechter & Yashar, 2021; Strasburger & Malania, 2013). Lastly, we examine how individual differences in crowding thresholds correlate across stimulus types and locations. Altogether, the results indicate that crowding affects the identification of letters differently than other stimuli with similar low-level visual features.

Methods

This study includes three experiments with similar methods. In the sections below, we first report the detailed methods in Experiment 1, then we highlight the differences in Experiments 2 and 3. Those sections are followed by a description of our analyses.

Experiment 1

Participants: 15 English-speaking volunteers were recruited from the Barnard College and Columbia University community of students and staff. Each participant gave informed consent in accordance with the Declaration of Helsinki and the Barnard College Institutional Review Board and participated in exchange for fixed monetary payment. All participants had normal or corrected-to-normal visual acuity. 13 were female and their mean age was 21 years (ranging from 19 to 31). One was ambidextrous and the rest were right-handed. All reported learning English before the age of 5, and all reported having no diagnoses of dyslexia or other learning disability. To assess reading skill we used the composite TOWRE-II Test of Word Reading Efficiency (Torgesen et al., 1999). All but one (with a score of 91) scored above the norm of 100 (mean = 112; SEM = 2.5).

The sample size was chosen in advance of data collection based on a review of similar published studies and our own pilot experiments. Shechter et al. (2024) investigated similar questions and based on a power analysis included 14 participants. We chose a target N=15.

Stimulus presentation: We used custom MATLAB software (MathWorks) and the Psychophysics Toolbox (Brainard, 1997; Pelli, 1997) to present stimuli on a ViewPixx 3D screen (VPixx Technologies) with a 120 Hz refresh rate and 1920 × 1080-pixel resolution. Participants sat with their head in a chinrest 60 cm from the screen. The background brightness was set to the screen's maximum of 100 cd/m2. An example trial is illustrated in **Figure 1.** A fixation mark was presented at the center of the screen throughout each trial. It was composed of a black cross 0.38 degrees of visual angle (º) wide, with a 0.1º white dot at its center, and a thin black ring around it (0.38º diameter).

The display also contained spatial cues to indicate the two potential target positions that were 4º to the left or right of the fixation point. The cue on each side was composed of two

vertical light green lines, each 0.1º thick and 0.6º long, one above the target location and one below. The endpoint of each line closest to the target position was 1.1º from the horizontal midline.

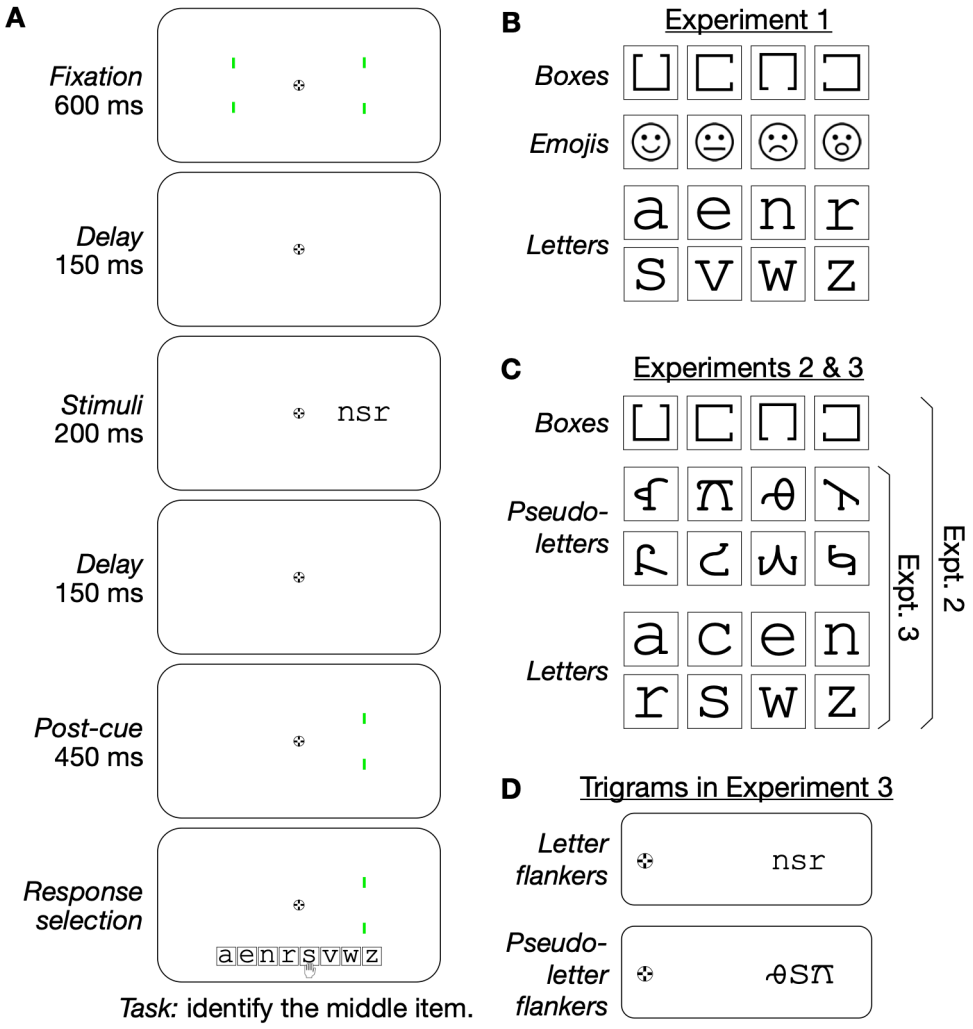

Figure 1: Stimuli and trial sequence. **(A)** Example trial sequence with a trigram of letters presented 4º to the right of fixation. **(B)** The individual stimuli presented in Experiment 1. **(C)** The individual stimuli presented in Experiment 2 & 3 (the boxes were not included in Experiment 2). **(D)** Example trigrams in Experiment 3, with a target letter either flanked by either letters or pseudo-letters. The stimuli are scaled such that the center-to-center spacing (as a fraction of the target's distance to the fixation point) matches the average crowding distance thresholds.

On each trial, we presented either a set of 3 shapes (i.e. a trigram) in a horizontal row, or a single shape, centered 4º directly left or right of the fixation mark. The side was randomized and unpredictable. There were three types of shapes, as illustrated in **Figure 1B:**

(1) *Boxes*: Black-framed squares, white on the inside, with a gap in one of the four sides. The outline thickness was 8.8% of the box's width. The gap was centered on one of the sides and occupied 31% of the side's length. The 4 unique boxes varied only in which side contained the gap (top, right, bottom or left).

(2) *Emojis:* Face icons that differed in the emotional expression. Each of the four unique emojis consisted of a black circle outline, two black dots for eyes, and a mouth. The outer line thickness was 5.6% of the face width, and the eye diameter was 15% of the face width. The shape of the mouth distinguished the emojis: an upwards curve for happy, and downwards curve for sad, a straight line for neutral, and an open oval for surprised. The four mouths were constructed to have approximately the same number of black pixels in all cases. The percentage of black pixels in each face image ranged from 18% to 19%.

(3) *Letters:* Black letters in the Courier New font: a, e, n, r, s, v, w, and z[1]. When adjusting the size of the letters to have a particular width in degrees, the letter "e" was taken as the standard. Thus, for all letters, to achieve a particular size for a particular target-flanker spacing level, we used the font size in points that made the tightest bounding box on the letter "e" subtend that width in degrees. The letter trigrams were chosen to exclude 13 familiar words: are, awe, ear, era, new, ran, raw, saw, sea, sew, war, was, and zen.

All individual stimulus items were equally likely to be the central target, each on the left and right side for an equal number of trials. On each trial, one item was chosen to be the central target and, on the 85% of trials with flankers, two others were randomly selected such that the trigram contained three unique items.

Trial sequence and procedure: Each trial began with the participant fixating on the central cross, with the green cues presented on both sides. Once their gaze position was verified (see details in the *Eye-tracking* section below), the trial began with a fixation interval of 600 ms. Then the cues disappeared, and after a delay of 150 ms containing only the fixation mark, the stimuli appeared, unpredictably on the right or left of fixation, with the middle shape centered 4º from fixation. On 85% of trials, the stimuli were a trigram of 3 shapes with variable size and spacing (as in Figure 1). On the remaining 15% of trials, only 1 target shape appeared with a fixed large width of 2.2º (the "*unflanked"* condition). The shape(s) were on the screen for 200 ms, after which only the fixation mark was presented for a delay of 150 ms. Then a post-cue appeared: one pair of green vertical lines centered on the target shape's location. This cue served to remove spatial uncertainty about which stimulus to judge. After 450 ms, the response selection display appeared. This consisted of the 4 or 8 stimulus alternatives, drawn in a horizontal row of black-framed rectangles 3º below the fixation

[1] For the first three participants tested, we used a "u" instead of a "v". For those participants, 3-letter words or acronyms containing a "u" were never presented: rue, run, sue, sun, urn, usa, and use. We then replaced the u with v to have fewer vowels in the set.

mark, with 1.8º between their centers. Each rectangle was 1.5º tall and 1.6º wide and contained one possible stimulus scaled to be 1º wide.

The participant then reported which target shape they had seen by clicking on it with the mouse. The cursor was displayed as a small hand icon. There was unlimited time to make this response. Immediately after the participant clicked on an item, the response alternatives disappeared and feedback for response accuracy was provided by a 100 ms tone played over speakers (600 Hz frequency for correct, 100 Hz frequency for incorrect). Then after a 500 ms delay, the next trial began.

Adaptive setting of stimulus spacing and sizes: For each trial with flankers, we chose a *spacing* level for the trigram, which is the distance between the centers of neighboring shapes, in degrees. The individual stimulus sizes were all scaled along with the spacing[2], such that the ratio of the spacing to the stimulus width was 1.25. 15% of trials used a trigram set to an "easy" level, with the stimulus width at 2.2º and the spacing at 2.75º. The purpose of these trials was to help us estimate the upper asymptotes of the psychometric functions.

On the remaining 70% of trials, the spacing (and item width) was controlled by an adaptive staircase procedure, in $\log_{10}$ units, using the Palamedes toolbox (Prins & Kingdom, 2018). The spacing recommended by the staircase increased after each incorrect response and decreased after each correct response. The step up was 0.108 log units and the step down was 0.046 log units. This ratio of step sizes up and down causes the staircase to converge at the 70% correct threshold. The minimum spacing was 0.19 degrees, and the maximum was 2.75 degrees. For each stimulus type and side, there were two randomly interleaved staircases, which ran throughout each testing session. One staircase started at a difficult spacing (0.28º) and one at an easy spacing (1.38º). The step sizes were halved after the third reversal.

Order of trial blocks: In Experiment 1, the stimulus types were presented in separate blocks of 40 trials. Blocks were run in sets of 3, each set containing one block for each stimulus type in a random order. Most participants completed the experiment over four one-hour sessions conducted on different days. The first session began with instructions and practice

[2] Scaling the stimulus size with the center-center spacing is a common approach to measure crowding (Kurzawski et al., 2023). In initial pilot experiments, we kept the stimulus size constant and varied the spacing only. This was problematic: in some cases, the size was too big, so the spacing could not be reduced enough to cause crowding. In other cases, the size was too small, and accuracy remained low even when the spacing was very large. We also tried to first calibrate the stimulus size to each participant's 99% correct threshold without flankers. (The data collected for this single-stimulus size manipulation are presented in the Supplemental Materials as Experiment S1). Nonetheless, when we added flankers, many psychometric functions of target-flanker spacing had poor upper asymptotes. That means that even when a target's size is well above the acuity threshold, introducing flankers at large distance (when crowding theoretically should be minimal) causes errors in target identification. Scaling the size and spacing together avoids this issue. In the Supplementary Materials we show that the stimulus sizes used at our critical spacing thresholds were far above acuity limits measured without flankers.

trials with each stimulus type, starting with unflanked targets at the maximum size, then the flanked (crowded condition) at the maximum size and spacing, and then smaller spacings under the control of the staircase. All participants then completed 60 experimental blocks of 40 trials, for a total of 2400 trials per participant. After excluding unflanked trials and fixation breaks (see below), each psychometric function was based on 338 trials on average.

Eye-tracking: We recorded the right eye's gaze position at 500 Hz with an Eyelink 1000+ video-based eye-tracker (SR Research). We performed a 9-point calibration at the start of each block. Fixation was established at the start of each trial. The trial only advanced if the estimated gaze position was within 1.5º horizontally and 2º vertically from the fixation mark for at least 200 ms. If this did not occur within 500 ms, the computer beeped to request fixation. If this happened more than twice, the program halted to re-calibrate the eye-tracker. Once fixation was established, the median estimated gaze position during the next 100 ms was defined as the "true" fixation position for that trial (allowing for some eye-tracker drift). Then, during the subsequent trial, the program detected fixation breaks online as follows: if at any point before the post-cue appeared, the estimated gaze position deviated by more than 1º from the "true" fixation position, the trial was immediately terminated. Text on the screen informed the participant they broke fixation and prompted them to press the space bar to continue to the next trial. Terminated trials were repeated at the end of the block, unless fewer than three trials remained. This applied to 12.7% of trials on average (SEM = 1.8%).

To be sure that we excluded trials in which participants may have looked directly at a target stimulus, we also analyzed the eye traces offline. Fixation breaks were defined as moments when the gaze position deviated for at least 30 ms by more than 1º horizontally or 2º vertically from the central gaze position (estimated as the median position during the initial fixation interval across trials). We detected additional fixation breaks in this offline analysis in only 0.5% of trials on average, and they were also excluded from the analysis.

Experiment 2

In Experiment 2, we replaced the emojis with pseudo-letters, which have visual features matched to Latin letters and provide a more controlled comparison of the crowding asymmetry. We also randomly intermingled the stimulus types within each block of trials. This meant that the participants could not predict the upcoming stimulus type, and any differences in crowding cannot be explained by differences in cognitive state (e.g., the distribution of spatial attention) when the stimuli appeared on the screen.

Participants: 15 new volunteers were recruited from the same population as in Experiment 1, with the same criteria and informed consent procedures. 10 were female and their mean

age was 21 years (ranging from 18 to 36 years). Their mean score on the TOWRE test was 116 (SEM = 3.1). All were right-handed native English speakers.

Stimulus presentation and procedures: All details of the stimuli and task were identical to Experiment 1 except as reported here. There were 3 stimulus types, as shown in **Figure 1C**:

(1) *Boxes:* The same 4 boxes as in Experiment 1.
(2) *Pseudo-letters:* 8 black characters in the BACS-2 serif font (Vidal et al., 2017), which are designed to match the size, symmetry, and number of strokes, junctions, and terminations of the corresponding characters in Courier New. The 8 characters displayed in BACS-2 corresponded to a, x, e, u, r, s, w, z. Six of these match the Courier New characters in the Letters stimulus set, but because the "c" and "n" in BACS-2 closely resembled many other characters, they were replaced with the more distinctive "x" and "u".
(3) *Letters:* The same 8 letters as in Experiment 1, except the letter "v" was replaced with a "c." Thus, the 8 letters in this set were: a, c, e, n, r, s, w, z. This change required excluding two additional three-letter English words from the trigram set: "can" and "car".

The trial sequence and task were identical to Experiment 1 (see **Figure 1A)**. But unlike Experiment 1, the stimulus types were randomly intermingled within each block, and there were no unflanked trials. Lastly, we reduced the total number of blocks per participant to 36, which they completed in 2-3 sessions each 30-45 minutes in length. This yielded an average of 234 trials per psychometric function.

Experiment 3

Experiment 3 was designed to test the hypothesis that the hemifield asymmetry is driven by a specific advantage for processing *strings* of familiar letters in the right visual field. We compared crowding distances for letter targets flanked by other letters, and letter targets flanked by pseudo-letters.

Participants: 15 new volunteers were recruited from the same population as in Experiments 1 and 2, with the same criteria and informed consent procedures. 12 were female and their mean age was 22 years (ranging from 18 to 36 years). Their mean score on the TOWRE test was 109 (SEM = 2.19). One was left-handed, and 12 were native English speakers. The remaining 3 were proficient English readers but had first learned Italian, Spanish or French.

Stimulus presentation and procedures: All details of the stimuli and task were identical to Experiment 2 except as reported here. The target stimuli were the same as the *Letters* set from Experiment 2, but there were now two flanker conditions, as illustrated in **Figure 1D.**

(1) *Letters flanked by letters:* this condition was identical to the Letters condition in Experiment 2.

(2) *Letters flanked by pseudo-letters:* each trigram contained a central target letter drawn from the same set of Courier New letters flanked by two different pseudo-letters. There were 8 possible flanker characters which had the same identities as in the Courier New letters set but presented in BACS-2.

The target hemifields and flanker types were randomly intermingled across trials of each block. Each participant completed 24 blocks of 40 trials over 2 or 3 testing sessions, yielding an average of 234 trials per psychometric function.

Analysis

Psychometric functions and crowding distances

We used the Palamedes toolbox (Prins & Kingdom, 2018) to fit one psychometric function for each participant, for each stimulus type and hemifield (left, right). **Figure 2** illustrates examples for one participant. Specifically, we fit a log-Weibull function *G* (also called a Gumbel function) to the binary response accuracies as a function of the $\log_{10}$ spacing (*s*) on each trial:

$$G(s) = \gamma + (1 - \gamma - \lambda)(1 - e^{-10^{\beta(s-\alpha)}})$$

The parameters are: α, the location (horizontal shift of the function); β, the slope; γ, the guess rate (the lower asymptote); and λ, the lapse rate (1 – the upper asymptote; i.e., the probability of an incorrect response independent of *s*). α was free to vary between -2 and 0.8. γ was fixed to 1/M, where M is the number of stimulus alternatives for that stimulus type (4 or 8). λ was constrained to be between 0 and 0.15.

To estimate β, the slope, we fit the two psychometric functions for each stimulus type twice: first, the slopes were free to range between 0.01 and 100. Then we fixed the slopes to be the average of the slopes for the left and right hemifields, for that participant, and fit again. This effectively reduced the degrees of freedom that could introduce noise in our primary measure of interest, the crowding distance threshold, which we label *d*. The slopes, when fit freely, did not reliably vary across hemifields.

The crowding distance thresholds *d* were defined as the center-to-center stimulus spacing predicted by the best-fitting function to yield an accuracy level *t* midway between chance (γ) and 1.0 (perfect). t=0.625 for stimulus types with 4 alternatives (boxes and emojis), and *t*=0.563 for stimulus types with 8 alternatives (letters and pseudo-letters).

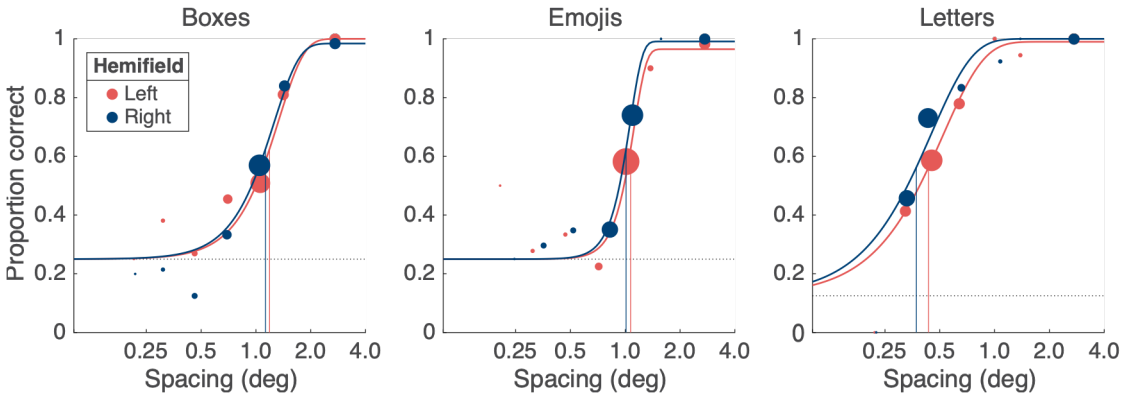

Figure 2: Example psychometric functions fit to a representative participant's data in Experiment 1. The dashed horizontal lines indicate chance accuracy, and the colored vertical lines are the crowding distance thresholds. The dots represent proportion correct in seven bins of log spacing, with the dot size scaled to the number of trials. These are for visualization only, as the psychometric functions were fit to the single-trial binary responses.

Analysis: Stimulus type and hemifield effects on crowding distances

To test hypotheses about crowding distances, we fit linear mixed effects models to individual distances (in $\log_{10}$ units) with fixed effects of stimulus type, hemifield, the stimulus-by-hemifield interaction, and random intercepts and slopes by participant. The model outputs are reported by MATLAB's fitlme function as the *F* tests from an ANOVA. We also computed, for each participant and stimulus type, the magnitude of the hemifield asymmetry as the *ratio* of the right crowding distance to the left crowding distance (d_R/d_L), with d_R and d_L in units of degrees (not logged). For these ratios, we fit a linear mixed effects model with a fixed effect of stimulus type, with random slopes and intercepts by participant. When there was a significant main effect of stimulus type, we conducted paired t-tests for each pair of stimulus types.

Analysis: Standardized Bouma factors

To facilitate comparison to other published studies, we also converted our crowding distance thresholds to a scale comparable to Bouma (1970), following the recommendations of Kurzawski et al. (2023). Specifically, we first transformed each fitted psychometric function *G* to normalize it by the guessing rate γ, the reciprocal of the number of stimulus alternatives (4 or 8).

The transformed function G* is:

$$G^* = \frac{G-\gamma}{1-\gamma}$$

We then calculated Bouma distance thresholds at an accuracy level based on Bouma's (1970) choice to calculate 75% correct thresholds (t=0.75) in a 25-alternative identification task (γ = 1/25 = 0.04). Transforming Bouma's t similarly to how we calculated G* gives us t^*:

$$t^* = (0.75 - 0.04) / (1 - 0.04)$$

$$= 0.74$$

The standardized distance threshold d^* is the $\log_{10}$ target-flanker distance when $G^* = t^*$. We then calculated the standardized Bouma Factor *b'* (Kurzawski et al., 2023), which is the standardized crowding threshold (in degrees, 10^{d^*}) divided by the target eccentricity (4º).

RESULTS

Our primary measure of crowding is the *crowding distance threshold*, or critical spacing, which is the distance between the centers of the target and the flankers at which accuracy reaches midway between chance and 100% correct. We estimated this distance threshold by fitting psychometric functions to each participant's single-trial responses, separately for each stimulus type and hemifield (see Figure 2 for example function fits).

Figure 3A plots crowding distances in each condition on a $\log_{10}$ scale. Each participant's thresholds are dots connected by a thin gray line, and the across-participant averages are represented by darker horizontal bars. **Figure 3B** plots the hemifield asymmetry for each stimulus type, expressed as the right:left ratio of the (not log-transformed) crowding distances. There is one column for each experiment in Figure 3.

Table 1 lists the mean crowding distances (in degrees) for targets of each type, along with statistics on the hemifield asymmetry (as a ratio). **Table 2** lists statistics on the comparisons of hemifield asymmetry magnitudes (as ratios) across stimulus types. For the same data expressed as the threshold target *size*, rather than target-flanker spacing, see Figure S1 and Table S1 in the Supplementary Materials.

Crowding distances in Experiment 1

In Experiment 1, we compared crowding distance thresholds across three stimulus types: trigrams of letters, emojis, and boxes. There was a main effect of stimulus type on the $\log_{10}$ crowding distances ($F(2,84) = 164.8$, $p<10^{-29}$), which were highest for boxes and lowest for letters. See Figure 3A, left panel. There was also a main effect of hemifield ($F(1,84)=9.67$, $p=0.003$), with generally higher thresholds in the left hemifield than the right. The interaction between stimulus type and hemifield was also significant ($F(2,84)=5.47$, $p=0.006$).

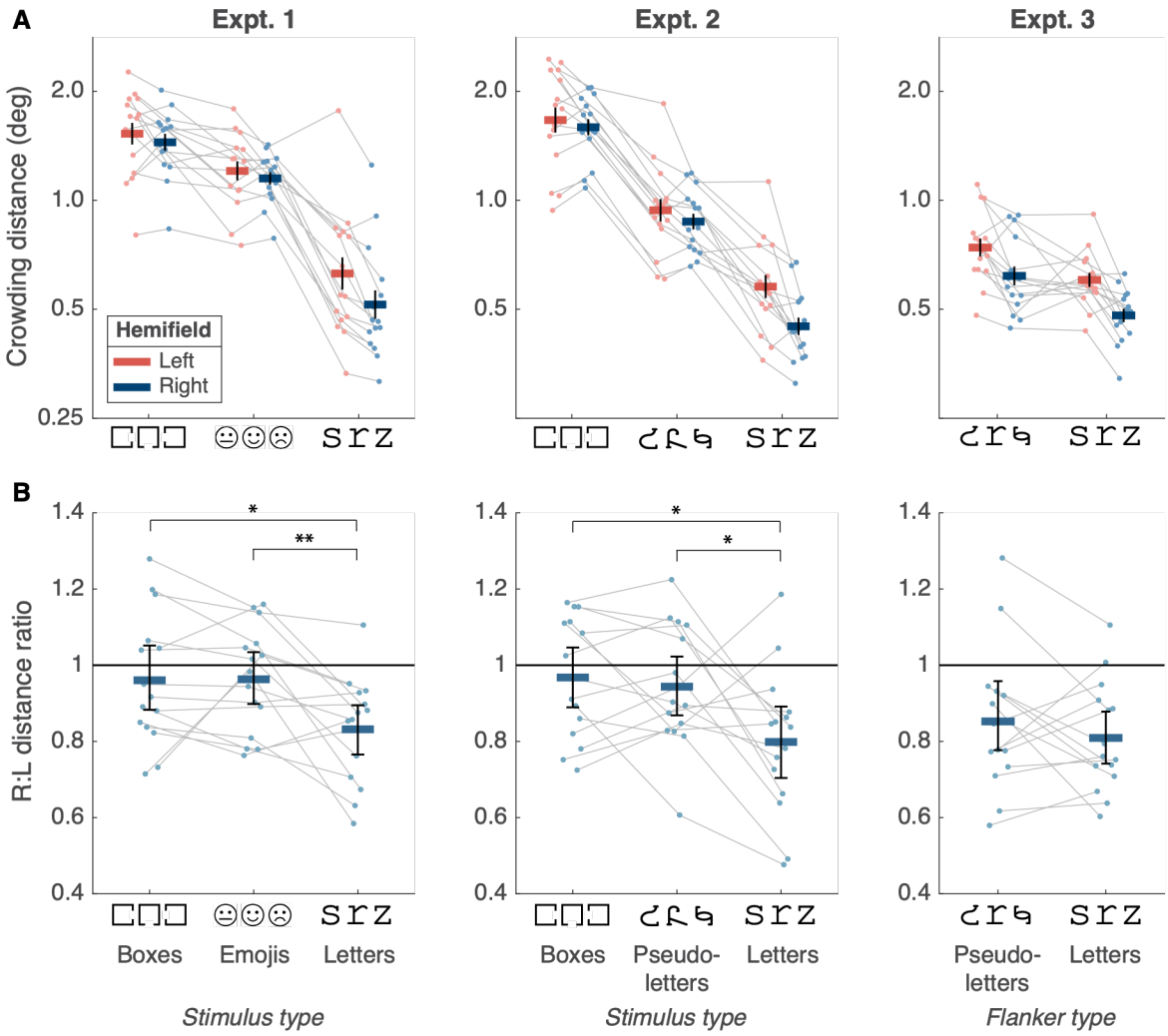

Figure 3: Crowding distances and hemifield asymmetries in each experiment. (A) Top row: crowding distance thresholds in degrees for each experiment, plotted on a $\log_{10}$ scale. Each point is one participant's distance threshold, and all points belonging to one participant are connected by a line. Red points are for targets in left visual field; blue for targets in right visual field. The darker horizontal lines are the across-participant means with error bars indicating +/- 1 SEM. **(B)** Bottom row: The hemifield asymmetries, expressed as the ratio of right:left crowding distances. Asterisks indicate significant pairwise differences in the hemifield asymmetry across stimulus types (* = p<0.05; **=p<0.01).

We then calculated the hemifield asymmetry as the ratio of right:left crowding distances, which adjusts for the different baseline thresholds across stimulus types. See Figure 3B, left panel. The asymmetry differed significantly across stimulus types ($F(2,42)=5.86$, $p=0.006$). As listed in Table 2, the asymmetry ratio was significantly larger for letters than emojis, and larger for letters than boxes, but not different between emojis and boxes. Evaluated separately, the right<left asymmetry was significant only for letters and not for boxes or emojis. That was true whether calculating the asymmetry as the difference between right

and left thresholds in units of degrees, as the difference in $\log_{10}$-transformed thresholds, or the ratio as plotted in Figure 3B and listed in Table 1.

			Mean crowding distance (deg)		Hemifield asymmetry (R:L ratio)				
Targets	**Flankers**	**Expt.**	***Left***	***Right***	***Mean [SEM]***	***95% CI***	***t(14)***	***p***	***BF***
Boxes	Boxes	1	1.58	1.48	0.96 [0.04]	[0.88 1.05]	-0.90	0.384	0.37
Boxes	Boxes	2	1.74	1.62	0.97 [0.04]	[0.89 1.05]	-0.79	0.442	0.34
Emojis	Emojis	1	1.24	1.16	0.96 [0.03]	[0.89 1.03]	-1.03	0.319	0.41
PL	PL	2	0.98	0.89	0.94 [0.04]	[0.87 1.02]	-1.36	0.195	0.57
Letters	Letters	1	0.69	0.55	0.83 [0.03]	[0.76 0.90]	-4.73	0.0003	103
Letters	Letters	2	0.60	0.46	0.80 [0.05]	[0.71 0.89]	-4.15	0.0010	39.1
Letters	Letters	3	0.61	0.49	0.81 [0.04]	[0.75 0.89]	-5.17	0.0001	212
Letters	PL	3	0.76	0.64	0.85 [0.05]	[0.77 0.96]	-3.10	0.0078	6.81

Table 1: Statistics on the mean crowding distances and the hemifield asymmetry expressed as the ratio of crowding distances in the right:left visual fields. The t-tests compare the asymmetry ratios to 1. The four comparisons that are bolded with $p<0.05$ remain significant after false discovery rate correction (Benjamini & Hochberg, 1995) for the eight tests in this table. Abbreviations: PL = pseudo-letters; SEM = standard error of the mean; CI = confidence interval; BF = Bayes Factor.

Crowding distances in Experiment 2

In Experiment 2, we compared crowding across three stimulus types: trigrams of letters, pseudo-letters, and boxes. The pseudo-letters were chosen to be matched to the letters in several visual features and in the number of target alternatives (8). They therefore provide a controlled comparison for the specificity of the hemifield asymmetry for legible letters.

We found a main effect of stimulus type on the $\log_{10}$ crowding distance thresholds ($F(2,84) = 188.1$, $p<10^{-31}$), which were highest for boxes and lowest for letters. See **Figure 3A**, middle panel. We also found a main effect of hemifield ($F(1,84)=11.4$, $p=0.001$), again with generally higher thresholds in the left hemifield. The interaction between stimulus type and hemifield was also significant ($F(2,84)=4.67$, $p=0.012$). Evaluated separately, the right<left asymmetry was significant only for letters and not for boxes or pseudo-letters (see Table 1).

The magnitude of the asymmetry (as a ratio) differed significantly across stimulus types ($F(2,42)=4.38$, $p=0.018$). As listed in Table 2, the ratio was significantly larger for letters than boxes, and larger for letters than pseudo-letters, but not different between pseudo-letters and boxes.

The difference between letters and pseudo-letters emphasizes that even when low-level visual features are well matched, the hemifield asymmetry is strongest for familiar letters.

Comparison	Expt.	Mean [SEM]	95% CI	t(14)	p	BF
Emojis - Boxes	1	0.00 [0.03]	[-0.05 0.08]	0.08	0.939	0.26
Letters - Emojis	1	-0.13 [0.04]	[-0.21 -0.06]	-3.26	0.006	8.85
Letters - Boxes	1	-0.13 [0.05]	[-0.23 -0.05]	-2.73	0.016	3.76
Letters - Boxes	2	-0.17 [0.06]	[-0.27 -0.03]	-2.81	0.014	4.24
Letters - PL	2	-0.15 [0.05]	[-0.24 -0.03]	-2.56	0.023	2.87
PL - Boxes	2	-0.02 [0.04]	[-0.10 0.04]	-0.64	0.530	0.31
Letter flankers – PL flankers	3	-0.04 [0.04]	[-0.13 0.04]	-1.02	0.326	0.41

Table 2: Statistics on *differences* between the hemifield asymmetry ratios across stimulus types in each experiment. PL stands for pseudo-letters. Negative numbers mean that there was a *stronger* asymmetry for the first stimulus type in the comparison. For example, in Experiment 1 the mean ratio for letters was 0.83 and the mean ratio for emojis was 0.96, for an average difference of -0.13. The four comparisons with $p<0.05$ remain significant after false discovery rate correction (Benjamini & Hochberg, 1995) for the seven tests in this table.

Crowding distances in Experiment 3

In the third experiment, we compared crowding for letters that are flanked by other letters versus for letters that are flanked by pseudo-letters. On the one hand, crowding is generally weakened when the flankers are visibly different from the target (Kooi et al., 1994; Manassi et al., 2012). Thus, any visual differences between the letters and pseudo-letters could lower crowding distances for pseudo-letter flankers. On the other hand, meaningful flankers (like letters) cause less crowding than meaningless shapes (Reuther & Chakravarthi, 2014). Thus, crowding distances could be lower overall when the flankers are letters than pseudo-letters. Moreover, the hemifield asymmetry for letter strings in Experiment 1-2 could be explained by devoted mechanisms to process strings of meaningful letters that may help the participant simultaneously identify the target and flankers that are also letters (Huckauf et al., 1999), specifically the right visual field. If so, then the hemifield asymmetry should be eliminated when a target letter is flanked by pseudo-letters.

We found a main effect of stimulus type on the $\log_{10}$ distance thresholds ($F(1,56) = 46.7$, $p<10^{-8}$), which were higher for pseudo-letter flankers than for letter flankers. See Figure 3A, right panel. There was also a main effect of hemifield ($F(1,56)=24.3$, $p<10^{-5}$), again with generally higher thresholds in the left hemifield than the right. The interaction between stimulus type and hemifield was not significant ($F(1,56)=0.87$, $p=0.35$). The right<left asymmetry in crowding distance was significant for both types of flankers, as listed in Table 1. The magnitude of the asymmetry ratio did not significantly differ between the flanker types, as shown in the last row of Table 2.

Thus, crowding is generally lowered when a target letter is flanked by letters, supporting a role for specialized mechanisms that reduce crowding for strings of familiar letters. In other words, strings of letters benefit from a "higher-level representation" (Huckauf et al., 1999). Meaningful flankers cause less crowding of letter targets (Reuther & Chakravarthi, 2014). However, this does not account for the hemifield asymmetry, which was roughly as strong when letters were flanked by pseudo-letters as by letters.

Standardized Bouma factors

To facilitate comparisons across stimulus types and previously published crowding distances, we rescaled our psychometric functions and distance thresholds following the recommendations of Kurzawski et al., 2023. See the Methods section for details. This approach accounts for differences in the guessing rate (determined by number of stimulus alternatives) and calculates distance thresholds comparable to the 75% correct thresholds in Bouma (1970). The standardized Bouma factor *b'* is the transformed distance threshold (in degrees) divided by the target eccentricity (4º). The results are plotted in **Figure 4,** with statistics in **Table 3.**

The results of this analysis were consistent with our primary analysis of crowding distances. The mean *b'* ranged from 0.18 for letters in the right visual field to 0.49 for boxes in the left visual field (averaged over experiments). The hemifield asymmetry was significant only for letter targets, and all differences in the asymmetry between letters and other target types were significant.

We can directly compare these data to Kurzawski et al. (2023). For letters with radial flankers, they found a right:left hemifield asymmetry of 0.78, which is just slightly stronger than our estimate of 0.81. However, our Bouma factors for letters in each hemifield – 0.23 on the left and 0.18 on the right – are lower than they reported: 0.31 and 0.24, respectively. Several differences between experiments could account for the discrepancy. Kurzawski et al. included both letters and digits in their stimulus sets, tested at 5º and 10º compared to our 4º, presented the stimuli for 150 ms compared to our 200 ms, and included fewer trials per participant. Bouma factors could be higher for digits, decrease with eccentricity (Kurzawski et al., 2023; Winsler & Luck, 2025), decrease with presentation duration (Coates et al., 2021), and decrease with training (Hussain et al., 2012; Yashar et al., 2015). Also, our participants had to monitor only two potential target locations that were marked by spatial cues (the green lines marking both locations in Figure 1A). That may have facilitated attentional selection of the target, improving accuracy and reducing distance thresholds.

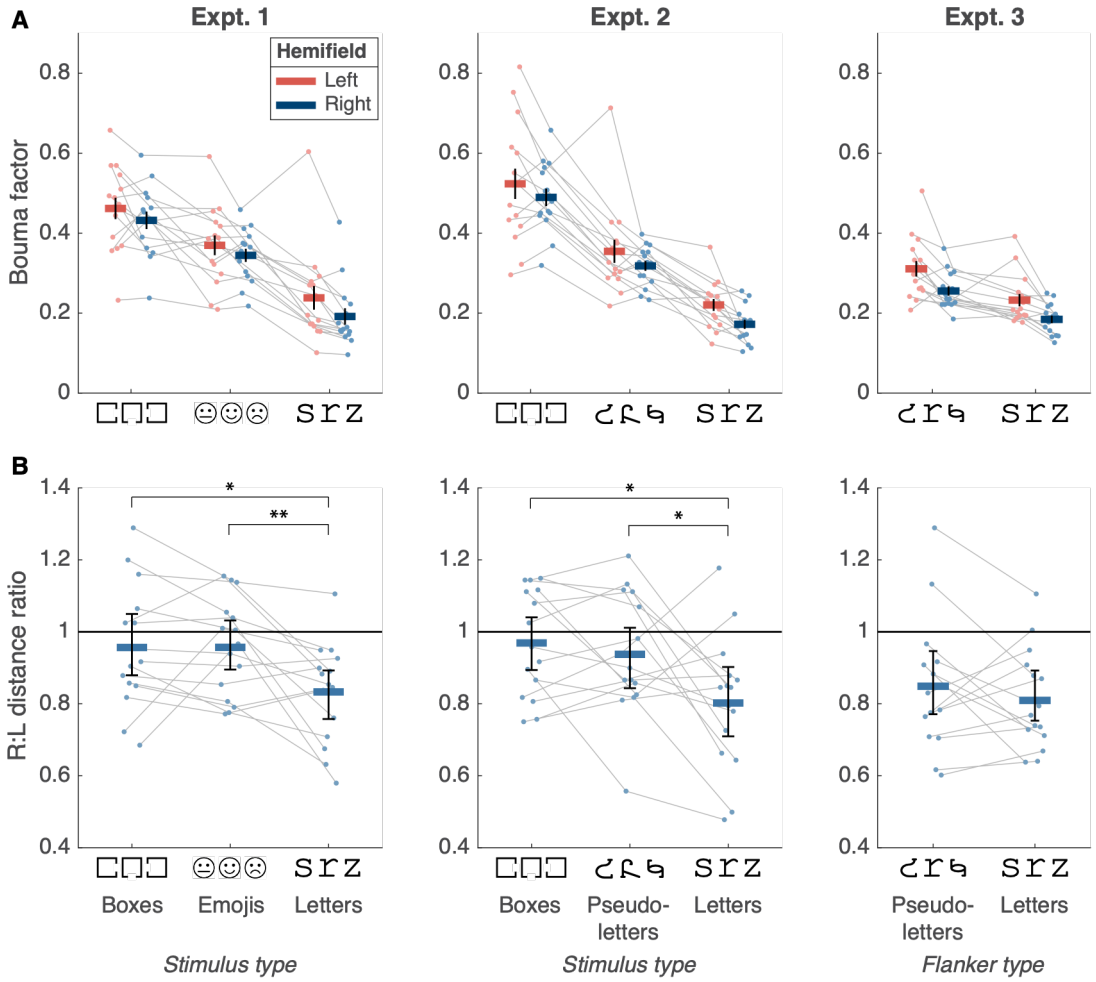

Figure 4: Crowding distances expressed as Bouma factors: standardized distance thresholds (correcting for the number of stimulus alternatives to be comparable to Bouma's (1970) thresholds) divided by the target eccentricity of 4º. Format as in Figure 3.

Lastly, the Bouma factors (b') can be used to estimate the width of the *visual span*, that is, how far out into the periphery crowded letters are legible (at Bouma's threshold of 75% correct). If we assume that *b'* is constant within each visual hemifield and constant across print sizes, we can calculate how far from fixation a letter trigram could be until the crowding distance is equal to one letter space. We define E_c as the critical eccentricity *in units of letter spaces* where the crowding distance is 1 letter space:

$$E_c = 1/b'$$

At that distance, half of each of the two outer letters fits within the "crowding zone" around the central letter. For the left hemifield, E_c = 1/0.23 = 4.4 letter spaces. For the right hemifield, E_c = 1/0.18 = 5.6 letter spaces. This matches other estimates of the visual span, which is said to encompass roughly 10 letters along the horizontal meridian and extends farther right than left (Legge et al., 2001).

			Mean Bouma Factor		Hemifield asymmetry (R:L ratio)				
Targets	**Flankers**	**Expt.**	***Left***	***Right***	***Mean [SEM]***	***95% CI***	***t(14)***	***p***	***BF***
Boxes	Boxes	1	0.46	0.43	0.96 [0.04]	[0.88 1.05]	-0.98	0.342	0.40
Boxes	Boxes	2	0.52	0.49	0.97 [0.04]	[0.90 1.04]	-0.80	0.435	0.35
Emojis	Emojis	1	0.37	0.34	0.96 [0.03]	[0.89 1.02]	-1.23	0.240	0.50
PL	PL	2	0.35	0.32	0.94 [0.04]	[0.85 1.02]	-1.43	0.174	0.61
Letters	Letters	1	0.24	0.19	0.83 [0.03]	[0.76 0.90]	-4.64	0.0004	89.1
Letters	Letters	2	0.22	0.17	0.80 [0.05]	[0.71 0.89]	-4.12	0.0010	37.3
Letters	Letters	3	0.23	0.18	0.81 [0.03]	[0.75 0.88]	-5.31	0.0001	264.7
Letters	PL	3	0.31	0.26	0.85 [0.05]	[0.77 0.95]	-3.19	0.0065	7.96

Table 3: Statistics on standardized Bouma Factors and the hemifield asymmetry in Bouma factors in each experiment. Formatted as in Table 1. PL stands for pseudo-letters.

Lapse rates

One advantage of measuring full psychometric functions is that we can distinguish true differences in crowding threshold – captured by horizontal shifts of the function – from differences in overall task ability or engagement – captured by shifts in the upper asymptote. The difference of the upper asymptote from 100% correct is the lapse rate, which is how often the participant makes an error even when the stimulus size and spacing are so large that crowding should not be a limiting factor (Prins, 2012).

In Experiment 1, we found that lapse rates differed significantly across stimulus types, being lower for letters than boxes and emojis ($F(2,84)=11.2$, $p<10^{-4}$). Lapse rates were also overall lower for stimuli in the right hemifield than the left ($F(1,84) = 5.14$, $p=0.026$). While Figure 5 suggests that this hemifield asymmetry in lapse rates was strongest for emojis and weakest for letters, there was no significant interaction with stimulus type ($F(2,84)=2.29$, $p=0.11$).

In Experiment 2, we also found that lapse rates differed significantly across stimulus types, being higher for boxes than pseudo-letters or letters ($F(2,84)=9.30$, $p<0.001$). However, there was not a significant difference between hemifields ($F(1,84)=0.034$, $p=0.85$), nor interaction with stimulus type ($F(2,84)=2.62$, $p=0.079$). Note that while for boxes and letters in Experiment 1 there was a trend for more lapses in the left hemifield, this trend was reversed in Experiment 2. This suggests that there is not a stable difference in the probability of a lapse across hemifields. Indeed, integrating the data for the boxes across all 30 participants in Experiments 1 and 2, there was no difference in lapse rates across the left and right hemifields (mean = 0.005, SEM=0.009, $t(29) = 0.61$, $p = 0.55$; BF = 0.23).

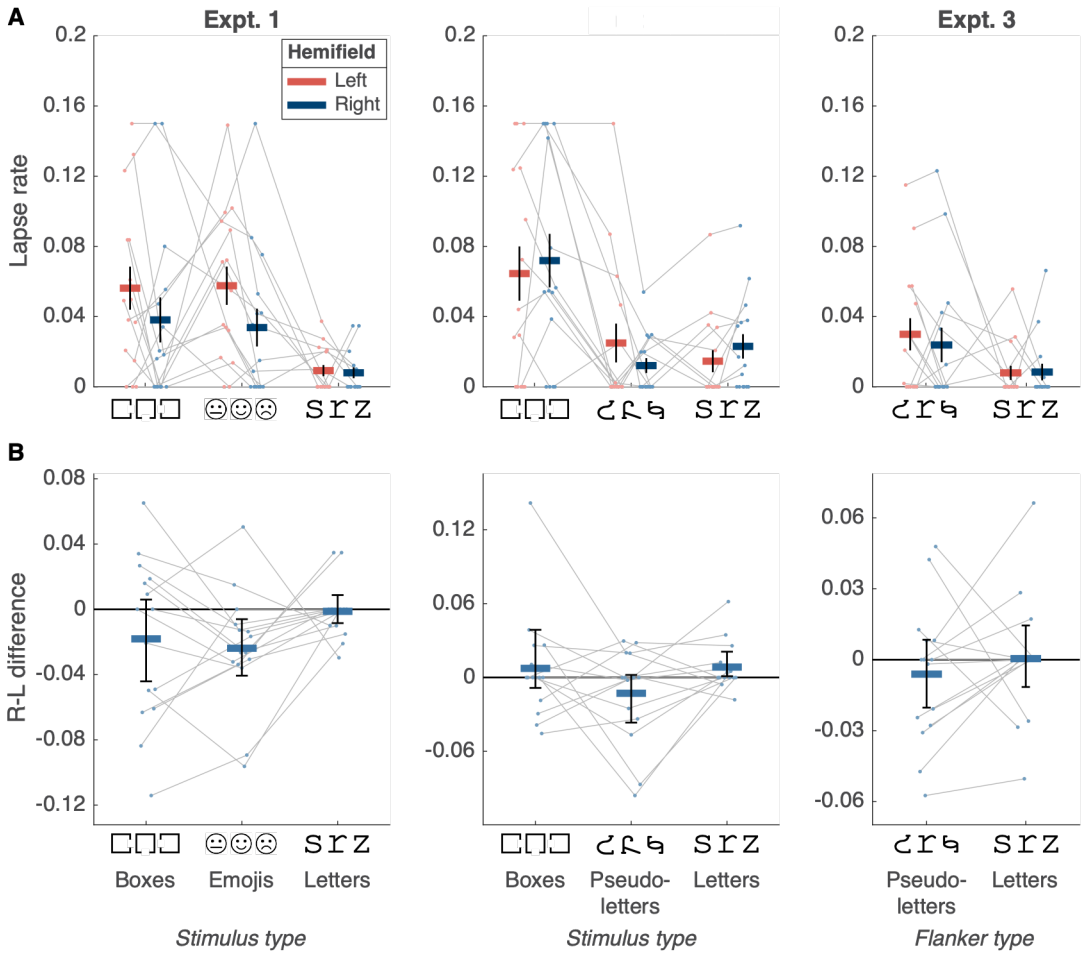

Figure 5: Lapse rates, which estimate the probability of an incorrect response even when the stimulus spacing is very high. Format as in Figure 3.

In Experiment 3, we found that lapse rates were significantly higher for letters flanked by pseudo-letters than for letters flanked by letters ($F(1,56)=4.40$, $p=0.036$), although lapse rates were low in both cases (on average below 5%). There was no effect of hemifield ($F(1,56)=0.28$, $p=0.60$), nor interaction between flanker type and hemifield ($F(1,56)=0.55$, $p=0.46$).

We conclude that the hemifield asymmetry for letters is not explained by an overall impairment on the left or more likely lapses of attention on the left, because lapse rates for letters were equally low in both visual fields. However, some stimulus types are more difficult than others to identify even when presented at a large size and with flankers at a large distance. Specifically, lapse rates were larger for boxes and emojis than letters. These errors are related to the presence of flankers, because accuracy was nearly perfect when the same large targets were unflanked. Letters may be spared this difficulty because each

is more visually distinct from the other and/or because participants are skilled at identifying and naming strings of letters.

Accuracy for uncrowded stimuli

Each participant in Experiment 1 also completed 60 "unflanked" or uncrowded trials for each stimulus type and hemifield. One target stimulus was presented alone at the maximum width (2.2º). These trials were randomly intermingled with the flanked trials. Average accuracy on the unflanked trials was between 99% and 100% correct for all conditions. The lowest accuracy scored by any participant in any one condition was 96.7% (two errors out of 60 trials). Thus, at the maximum size we used, the target stimuli were all very easy to identify. Errors were caused by crowding when flankers were present.

In a separate experiment, we measured *unflanked size thresholds* for boxes, emojis and letters each presented alone. In the **Supplemental Materials** we present the data from this experiment, which we label Experiment S1, and compare it to Experiment 1's size thresholds (which are equal to the crowding distance thresholds divided by 1.25).

The data show that the uncrowded size thresholds (in Experiment S1) were much smaller than the crowded size thresholds (in Experiment 1 with flankers). The mean uncrowded vs. crowded size thresholds in the left hemifield for each stimulus type were: boxes: 0.18º vs 1.26º; emojis: 0.53º vs 0.99º; letters: 0.21º vs 0.55º. Thus, the stimulus sizes at the crowding distance thresholds in Experiment 1 were far above the acuity limits measured in Experiment S1 (no flankers). Performance in Experiment 1 was therefore limited by crowding. Note that this comparison is not perfect because the stimulus protocol differed in Experiment S1: the target duration was 150 ms rather than 200 ms, and there were no spatial cues. However, these differences likely increased the task difficulty in Experiment S1, but nonetheless size thresholds were much smaller.

The data also show that the perceptual limits imposed by crowding and acuity are distinct. While boxes had the highest thresholds of the three stimulus types when crowded (as shown in Figure 3A, left panel), boxes had the lowest size thresholds when uncrowded. In other words, acuity is very good for localizing the small gap on the side of a single box. But when flanked by two other boxes with different orientations, the target must (on average) be scaled by a factor of 7 to achieve the same accuracy. In contrast, for emojis, the average crowded size threshold was only 1.9 times the average uncrowded size threshold. For letters, that scale factor was 2.6. We suggest that the crowding effect is stronger for boxes because all the alternative targets are rotations of the same shape, whereas each letter is a distinct shape with a distinct name, which ameliorates the perceptual uncertainty caused by crowding.

Curiously, we also observed a hemifield asymmetry for single uncrowded letters: smaller size thresholds in the right visual field than the left. There was no such asymmetry for boxes or emojis. The asymmetry for uncrowded letters was statistically significant and relatively consistent across observers (14/15 had a ratio less than 1), but quite small: the average right:left ratio of size thresholds was 0.95 (a 5% improvement on the right) as compared to the mean of 0.83 for crowded letters (a 17% improvement on the right). We therefore hesitate to conclude that the right visual field advantage for letters has a strong impact on acuity or perception of single letters, but it should be investigated further.

Errors in which the participant reports a flanker

In this analysis, we probe how crowding differs across stimulus types and hemifields by computing how often errors are reports of a flanker. These "substitution" or "mislocalization" errors are informative as to the underlying mechanisms of crowding (Freeman et al., 2012; Huckauf & Heller, 2002; Shechter & Yashar, 2021; Strasburger & Malania, 2013).

When the participant makes an error, they could either report the item that was the *outer flanker* (to the left of a target in the left hemifield; to the right of a target in the right hemifield), the item that was the *inner flanker* (vice versa), or they could report an item that was neither flanker (an intrusion or misidentification error). Inequalities between the probability of reporting the inner vs. outer flanker can be related to the inner-outer asymmetry of crowding: flankers more eccentric than the target cause more errors in than flankers closer to the fovea (Banks et al., 1977; Bouma, 1973; Levi, 2008; Mackworth, 1965).

In this analysis, for each stimulus type, hemifield, and participant, we analyzed trials in which the target-flanker spacing was within 0.3 log units of the participant's crowding distance threshold for that condition. This selects trials in which crowding made the target difficult, but not impossible, to identify. Accuracy on these trials was 60% correct, averaging across conditions (ranging from 55 to 64% across stimulus types and sides). Within these near-threshold trials, we first excluded all trials with correct responses and then tabulated the proportions of errors that were reports of the outer flanker, the inner flanker, or an item that was not a flanker. The results are plotted in **Figure 6**.

Note that even if the participant makes completely random guesses, the probability of a substitution error differs across the stimulus types with different numbers of possible targets, M. In each panel of Figure 6, a dashed horizontal line that marks the probability p_F of an error that is a report of a flanker by random chance. The number of items that could be selected is M-1 (given that the target was not selected). Thus, p_F=1/(M-1). When M=4, p_F=0.33. When M=8, p_F=0.14. The solid horizontal line marks p_N, the probability of an error

that selects *neither* flanker by chance: p_N=(*M*-3)/(*M*-1). The numerator is the number of items that were not presented, *M*-3. When *M*=4, p_N=0.33, and when *M*=8, p_N=0.71.

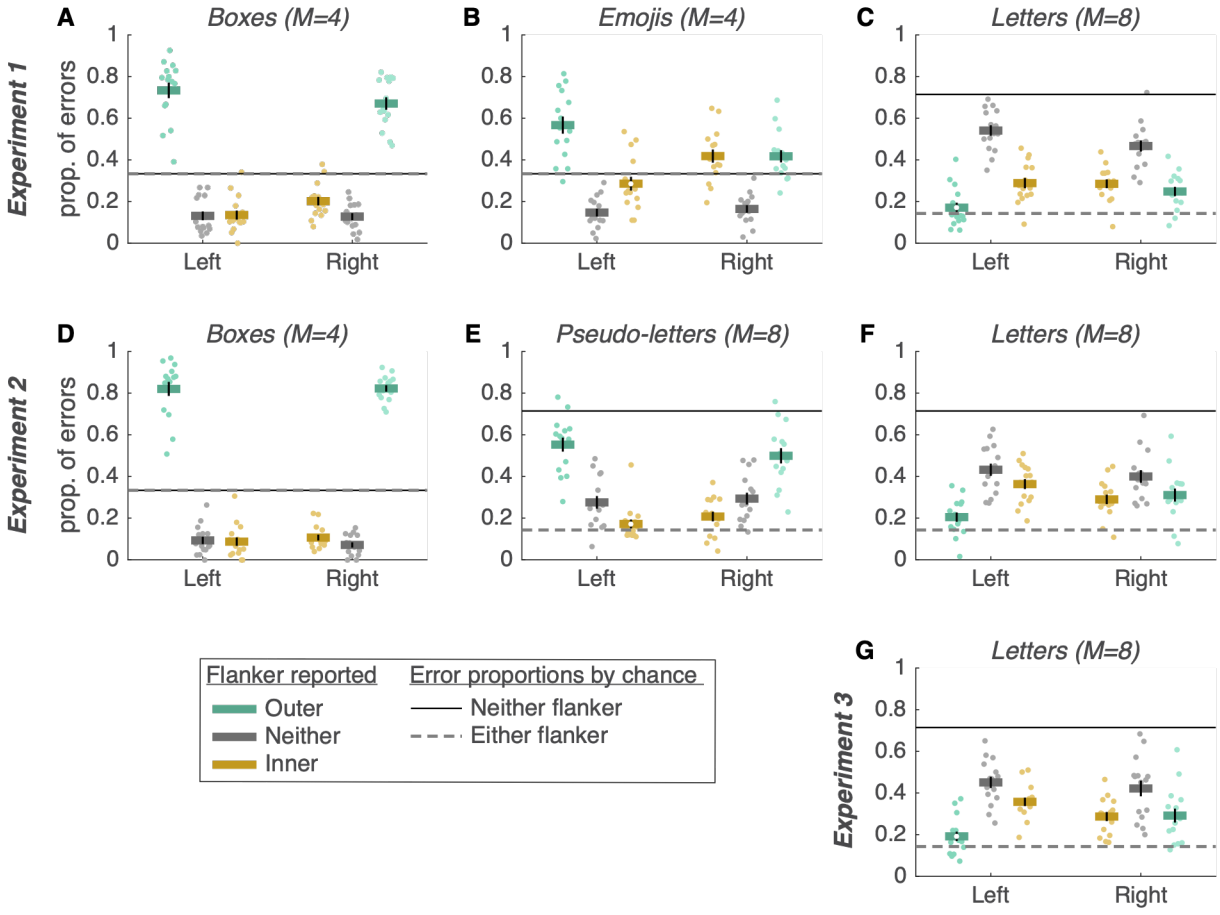

Figure 6: Analysis of errors. Each row corresponds to one experiment, and each panel corresponds to one stimulus type. *M* is the number of alternative targets. The y-axis is the proportion of errors in which the participant made a certain type of response. The data are grouped by target hemifield (left vs. right) along the x-axis. Dots are data for individual participants, and the horizontal bars are the means with +/- 1 SEM error bars. The horizontal solid line marks p_N, the probability that the participant would select neither flanker by chance. The horizontal dashed line marks the p_F, the probability that the participant would select either of the flankers by chance. p_N and p_F vary with *M*. For each error type, a small white dot on top of the mean bar indicates that it did *not* differ significantly from the level predicted by chance. The data from Experiment 3 for letters flanked by pseudo-letters are not included here, because pseudo-letter flankers could not be selected by the participant.

Thus, some differences across stimulus types in the patterns of errors can be attributed to these different baseline probabilities expected even by chance. Nonetheless, in 38 of the 42 conditions tested in Figure 6, the probability of each error type differed significantly from the level expected by chance (p-values corrected for false discovery rate). The remaining 4

conditions are marked by small white dots. Thus, participants were more likely to make substitution errors than expected by chance.

Figure 6 also shows striking differences in the proportion of errors that are reports of an inner vs. outer flanker. For boxes, emojis, and pseudo-letters, the most common errors are reports of the outer flanker. This has been reported before (Estes et al., 1976; Shechter & Yashar, 2021; Yashar & Carrasco, 2024). For boxes, among trials in which one flanker was reported, the average probability of selecting the outer flanker ranged between 0.77 and 0.90 (across experiments and sides). This bias for selecting an outer flanker did not differ across hemifields for boxes or pseudo-letters, but for emojis it was significantly weaker on the right ($t(14)=3.0$, $p=0.01$). For none of these non-letter stimulus types did the probability of selecting a non-flanker differ across sides (all *$p>0.37$, $BF<0.38$)*.

For letters, the pattern of errors is different. First, substitution errors are less common: participants are less likely to report a flanker and more likely to report an item that was not presented. This comparison is clearest for letter targets vs. pseudo-letter targets in Experiment 2 (both M=8). Compare the gray bars in panels E and F. The probability of reporting a non-flanker was significantly higher for letters than pseudo-letters ($F(1,56)=21.5$, $p<10^{-4}$), but did not differ across hemifields ($F(1,56)=0.24$, $p=0.63$), nor was there an interaction between hemifield and stimulus type ($F(1,56)=1.08$, $p=0.30$). This result suggests that letters benefit from more precise spatial coding, such that a greater proportion of errors are genuine misidentifications rather than positional errors.

Second, for letters, substitution errors were less likely to be reports of the outer flanker than they were for other stimulus types (compare the green and yellow data points in Figure 6). In Experiments 1 and 2, the *proportion of substitution errors* in which the outer flanker was selected differed significantly across stimulus types ($F(2,84)=59.7$, $p<10^{-16}$; $F(2,84)=95.5$, $p<10^{-21}$, respectively).

Third, for letter targets, the bias to select inner vs. outer flankers differed across hemifields. In Experiments 1 and 2, the proportion of outer-flanker substitution errors was affected by an interaction of stimulus type and hemifield ($F(2,84)=6.20$, $p=0.003$; $F(2,84)=4.91$, $p=0.01$, respectively). For letters, when the target was on the left, participants were more likely to select the *inner* flanker than the outer flanker, but when the target was on the right, they had no significant bias. The difference across sides in terms of the bias to pick the outer flanker was nearly significant in Experiment 1 ($t(14)=1.92$, $p=0.08$), and significant in Experiments 2 ($t(14)=3.11$, $p=0.008$) and 3 ($t(14)=3.30$, $p=0.005$).

These results are not entirely in agreement with two previous studies. One noted that with trigrams of digits in the right visual field, erroneous reports of the inner (leftmost) flanker were most common, in contrast to the outer-flanker bias observed for other stimulus types

(Strasburger & Malania, 2013). Another study using trigrams of letters found a general bias to report the leftmost letter in *both* visual fields, and attributed that to a left-to-right selection process (Huckauf & Heller, 2002).

Overall, these patterns of errors demonstrate that crowding works differently for letters than other types of stimuli. For non-letters, most errors are driven by reporting the outermost flanker instead of the target. But for letter trigrams, participants largely avoid the tendency to report the outer flanker, even though the outer flanker is the least crowded. This may reflect a difference in guessing strategy when the target cannot be identified.

However, the patterns of errors do not on their own explain why, for letters, crowding thresholds are lower in the right visual field than the left. If the reduced probability of reporting the outer flanker helped reduce crowding for letters overall, then we would expect that outer-flanker reports would be least likely for letters on the right, which is not the case. To explain these results, we need a more complete model that includes feature integration, positional uncertainty, and guessing strategies.

Individual differences in crowding thresholds and correlations across stimulus types

Crowding thresholds differed widely across individuals in our sample, although they were all healthy young adults with normal vision and good reading skills. In a final analysis, we investigated whether these individual differences generalize across stimulus types and hemifields. For instance, if an individual has low crowding for letters in the right visual field, will they also have low crowding for boxes in the right visual field, or letters in the left visual field? Correlations between conditions can illuminate the underlying factors that determine how well each participant is able to perceive each stimulus.

In the **Supplementary Materials** we present a full analysis of these individual differences. The conclusions are as follows:

(1) Crowding distance thresholds varied widely across individuals, with high test-retest reliability. For example, across the 30 participants in Experiments 1 and 2, crowding distances for letters in the right hemifield ranged from 0.31º to 1.25º. Thresholds fit to even-numbered trials correlated well with thresholds fit to odd-numbered trials (r=0.87).

(2) We found significant correlations even for pairs of conditions that differ in both the stimulus type and side. These correlations could be due to factors that generally influence task performance, such as the degree to which the participant is engaged in the task.

(3) Individual variation in crowding thresholds is also stimulus-specific. Crowding thresholds for one condition correlate better with thresholds for the same stimulus type in the opposite hemifield than for a different stimulus type in the *same* hemifield. This is not

consistent with a simple model of crowding caused by a low-level mechanism that integrates features of all stimuli present within certain portions of the visual field. Despite having matched visual features, crowding for pseudo-letters correlated worse with letters than with boxes.

(4) The data also suggest, tentatively, that there are hemifield-specific crowding mechanisms that partially generalize across stimulus types. When crossing stimulus types (e.g. letters vs. boxes), correlations tended to be higher for the same side than across sides, although those comparisons were not statistically significant. In Experiment 3, correlations were higher for different flanker types on the same side than the same flanker type across sides. Thus, crowding for letters differs in reliable ways across the hemifields.

(5) The hemifield *asymmetries* (right:left ratios of crowding distances) correlate moderately well across various types of stimuli, *except* for letters. Therefore, these data suggest that the right visual field advantage for letters has a unique cause.

We caution against drawing strong conclusions from these exploratory analyses of individual differences, which must be further tested with larger sample sizes. Nonetheless, they support the hypothesis that crowding differs idiosyncratically across individuals and systematically across stimulus types. As explained in the next section, we propose that the severity of crowding is influenced not only by general low-level visual factors but also by shaped by experience and expertise with particular stimulus categories.

DISCUSSION

Summary

We found that the right visual field advantage for crowding is specific to familiar letters. This hemifield asymmetry means that letters must be closer together to crowd each other in the right visual field than the left. There was a slight trend for a hemifield asymmetry in the same direction when the stimuli were simple boxes, emojis, or unfamiliar pseudo-letters with similar visual features. However, these asymmetries were much smaller than for letters, and more variable across participants. Averaging across experiments, the ratios of crowding distances in the right:left visual fields were: 0.82 for letters; 0.96 for boxes; 0.96 for emojis; and 0.94 for pseudo-letters. Put another way, for letters, crowding was 18% weaker on the right side of fixation than the left side, but for the other stimulus types this difference was only 4-6%. Thus, the hemifield asymmetry for letters is at least three times as large as for other stimulus types, even those with very similar visual features.

Moreover, none of the non-letter hemifield asymmetries were statistically significant. To gain power, we integrated the crowding distances for the box stimuli across Experiments 1 and 2, yielding asymmetry ratios for 30 participants. The mean ratio was 0.964 (SEM=0.029),

which did not differ significantly from 1 ($t(29) = -1.22$, $p = 0.23$; BF = 0.380). For a t-test to have 90% power to detect a significant asymmetry with this measured mean and standard deviation, 206 participants would be required (each with over 450 trials). Thus, this dataset demonstrates that for simple shapes that are not letters, the hemifield asymmetry is very small and might not be distinguishable from 0.

The other findings in this study were:

(1) Crowding distances were much lower for letters than all other stimulus types tested (contrary to Wallace & Tjan, 2011). That difference is not explained by better acuity for letters, which had larger unflanked size thresholds than did boxes. Moreover, accuracy was nearly perfect for all stimulus types and locations when a single item was presented at a supra-threshold size without flankers.
(2) The hemifield asymmetry for letters persisted when letter targets were flanked by unfamiliar pseudo-letters rather than other letters. Therefore, the right visual field advantage is not due to a left hemisphere superiority for processing strings of letters and precisely coding their positions.
(3) However, crowding thresholds were elevated on both sides when letters were flanked by pseudo-letters as compared to flanked by letters. This is consistent with previous reports that unfamiliar or meaningless flankers produce more crowding (Huckauf et al., 1999; Reuther & Chakravarthi, 2014).
(4) The Bouma factors for letters are consistent with a "visual span" that can encompass 10 characters and extends farther to the right than left of fixation.
(5) Lapse rates were lower for letters than other stimulus types; in other words, the psychometric functions' upper asymptotes reached closer to 100% correct for letters. However, the hemifield asymmetry for crowding distance thresholds was not mirrored by a hemifield asymmetry in lapse rates.
(6) For non-letter targets, most errors were substitution errors: reports of a flanker's identity, and most of those were reports of the outermost flanker. For letter targets, substitution errors were less common, and in the left visual field, reports of the *inner* flanker were more likely. In the right visual field, erroneous reports of the inner or outer flanker were roughly equally likely.
(7) Despite good split-half reliability, individual differences in the hemifield asymmetries for letters did not correlate well with the asymmetries for other stimulus types.

Comparison to previously reported hemifield asymmetries

A recent summary of the literature by Kurzawski et al. (2023) provides hemifield asymmetries that are similar to what we found; namely a significant asymmetry for letters (a right:left ratio near 0.8) and no significant asymmetry for non-letters. The non-letter data they summarized came from Greenwood et al. (2017): "tumbling clock" stimuli had a

weaker right:left asymmetry of 0.91 that did not significantly differ from 1. Note that a lower ratio is a stronger asymmetry.

Other relevant studies have not measured crowding distances but compared accuracy levels for crowded letters vs. other stimulus types, across hemifields. Two are suggestive of a larger right visual field advantage for letters as compared to symbols (Chanceaux & Grainger, 2012), and as compared to simple outline shapes (Chanceaux et al., 2013).

We are aware of only two studies that directly compared crowding distance thresholds for letters vs. other stimulus types within the same participants with similar task procedures. Grainger et al. (2010) compared letters with non-letter symbols (Σ, <, Ψ, &, @, £, ∞, λ, Π, ♂). Thresholds were lower for letters than symbols, and lower in the right visual field than the left. The average magnitude of that asymmetry was stronger for letters than symbols (the right:left ratios were 0.67 and 0.79, respectively). There was, however, no significant interaction between visual field and stimulus type. More recently, Winsler and Luck (2025) compared upright letters to inverted letters, and upright letters to Gabor patches. They also found that the hemifield asymmetry did *not* significantly differ across stimulus types.

Why did we find a significantly stronger asymmetry for letters than other stimulus types, unlike to those two studies? First, all of the symbols in Grainger et al. (2010) were meaningful and often co-occur with letters in text, unlike the false fonts and boxes in our experiments. Second, the stimulus durations were shorter in both previous studies: 80 ms in Grainger et al. and 100 ms in Winsler & Luck, compared to our 200 ms. Perhaps increasing the stimulus duration disproportionately improves processing in the left visual field – unless the stimuli are letters, which have a more stubborn asymmetry.

Third, we estimated crowding distances in a different way, by fitting full psychometric functions that allowed for differences in slope and lapse rate. Grainger et al. (2010) do not specify those details of their fitting procedure. Winsler and Luck (2025) used an adaptive staircase that assumes a fixed slope and lapse rate. Their lapse rate was 0.02, which may be an underestimate. Moreover, both previous studies fixed the stimulus size and varied spacing only, while we scaled the stimulus size and spacing together. In a pilot test, we found that with a fixed size well above the acuity limit, lapse rates exceeded 0.10 in many cases. Therefore, some of the apparent differences in crowding thresholds reported by previous studies may have been driven by differences in the upper asymptote rather than the threshold *per se*.

Lastly, Cutler et al. (2024) compared accuracy for reporting a letter in a string that formed either a real word or a pseudoword. They found a right visual field advantage only for letters in real words. That is not consistent with the clear right visual field advantage for letters in

non-words that we and others have found. Note that their targets were at a large eccentricity (9º) and the intra-letter spacing never went below 20% of the eccentricity.

Can the hemifield asymmetry be explained by asymmetric spatial attention or sensitivity to high spatial frequency?

Our crowding tasks are attentionally demanding; they are essentially parafoveal versions of the classic flanker task (Eriksen & Eriksen, 1974), in which task-irrelevant flankers can affect judgements of a central target. Moreover, pre-cueing covert spatial attention to a target reduces the crowding distance (Harrison et al., 2013; Kewan-Khalayly et al., 2022; Yeshurun & Rashal, 2010). Pre-cueing attention also results in a greater *improvement* for identifying a target letter in the left visual field than in the right (Ramamurthy et al., 2021). A similar pattern has emerged for words (Ducrot & Grainger, 2007). In principle, therefore, in the absence of any spatial cues, an unequal distribution of covert spatial attention could contribute to a hemifield asymmetry of crowding distances. Evidence for hemifield asymmetries of spatial attention in neurotypical individuals is decidedly mixed, with some claims of biases to the left and others to the right (e.g., Arguin et al., 1990; Carlei & Kerzel, 2018; Evert et al., 2003; Meyyappan et al., 2023; Michael & Ojéda, 2005; Ransley et al., 2018).

Regardless, given our experimental design, the crowding asymmetry for letters is not easily explained by a rightwards bias of spatial attention because it is stimulus-specific, even when the stimulus types and locations are randomly intermixed. If there was an attentional bias to the right, it should equally affect all stimulus types, especially when it is not possible to predict which type of stimulus will be flashed next. Also, lapse rates were equally low for letters in both hemifields.

We make a similar argument to rule out explanations based on a general right visual field advantage for the "local" elements of a stimulus array (Brederoo et al., 2017) or for processing high spatial frequencies (Peyrin et al., 2003; Sergent, 1982). First, it is not clear how this difference would affect the processing of letter strings specifically (Tadros et al., 2013). Moreover, the letters and pseudo-letters in our stimulus sets were similar in low-level features and yet differed in the hemifield asymmetry. Emojis did not have a significant asymmetry for crowding distances, but they seem to have contained the finest spatial details because in Experiment S1 they had the largest unflanked size thresholds. Thus, the letter-specific right visual field advantage is unlikely to be explained by lateralized sensitivity to high spatial frequency.

Interpretation: A modified receptive field hypothesis

To explain our results, we propose that reading experience strengthens connections between left hemisphere language areas and the left hemisphere visual areas that identify shapes. Language processing is left-lateralized in most people, and learning to read

develops a text-selective region that is usually more pronounced in the left ventral occipito-temporal cortex (Dehaene et al., 2010; Dehaene-Lambertz et al., 2018; Nordt et al., 2021; Pegado et al., 2014). This 'visual word form area' is thought to efficiently process letter strings and communicate with higher-level language areas to identify words. The effects of learning to read might also extend farther "down" into the visual hierarchy (Chang et al., 2015; Dehaene et al., 2015), affecting retinotopic regions where receptive field sizes determine crowding zones for single letters. V4 is a candidate region for letter crowding, for instance (Kurzawski et al., 2025).

We hypothesize that literacy experience develops populations of neurons that identify letters at specific visual field positions. These "letter detectors" efficiently process horizontal strings of letters in parallel (Grainger et al., 2016). Developing these detectors relies on connections to higher-level language areas, which are typically left-lateralized. As a result, the letter detectors have more precise spatial tuning (i.e., narrower receptive fields) in the left hemisphere, which causes smaller crowding distances in the right visual hemifield. As Bouma (1973) said, "The [right] field advantage may be due to a smaller range of interference."

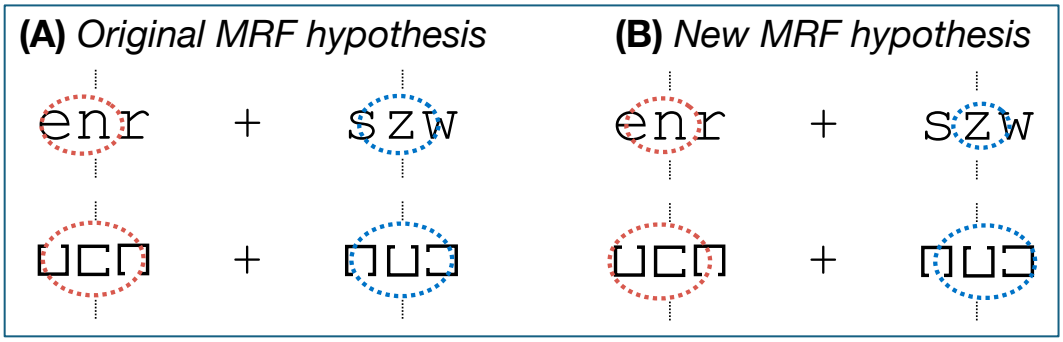

Figure 7: Modified receptive field (MRF) hypotheses. (A) The original MRF hypothesis (Tydgat & Grainger, 2009; Grainger et al., 2010; Chanceaux et al, 2013). The top row illustrates crowded letter trigrams to the left and right of a central fixation mark. The bottom row illustrates crowded boxes at the same positions. The dashed vertical lines mark the horizontal positions of the target. The dashed ellipses represent the receptive fields (RFs) of neurons that are critical for identifying the central target. Crowding occurs if a flanker intrudes upon this RF. In the original MRF hypothesis, neurons tuned to letters have generally smaller RFs than neurons tuned to other categories. In the left visual field, letter-tuned RFs are shifted to the left, causing more crowding by the leftmost flanker. **(B)** Our new MRF hypothesis. Neurons tuned to letters have smaller RFs than neurons tuned to other categories, but all RFs extend farther into the periphery than towards the fovea. The hemifield asymmetry is explained by the smaller RF in the right visual field only for letters (which is not drawn to scale here).

Our model is similar in some regards to the "modified receptive field (MRF) hypothesis," which was proposed to account for differences in crowding between letters and symbols

(Chanceaux et al., 2013; Grainger et al., 2010; Tydgat & Grainger, 2009). (For a different view, see Castet et al., 2017). See **Figure 7A.** There are two key properties of the original MRF hypothesis, which focuses on the receptive fields of hypothetical letter detectors in visual cortex: (1) letter detectors have smaller receptive fields than do the mechanisms that identify non-letter stimuli; (2) In the left visual field, the letter detectors' receptive fields are shifted leftwards. The first property explains why crowding distances are smaller for letters than other stimuli, as we also found. The second property accounts for preferential processing of the first letter in a string presented to the left visual field.

The original MRF hypothesis does not address the hemifield asymmetry we observed. Therefore, in our new MRF hypothesis (**Figure 7B)**, letter detectors along the horizontal meridian have smaller receptive fields in the right hemifield than in the left. This reduces the deleterious influence of flanking letters or similar shapes. These letter detectors in *both* hemifields also have smaller receptive fields than do the mechanisms that identify other types of stimuli.

Note that the ellipses in Figure 7 need not necessarily represent receptive fields of single neurons; they could represent the summed "integration zone" zone in which a *population* of neurons analyzes visual features to identify the central target.

The original MRF hypothesis also does not easily explain our pattern of substitution errors: for non-letter stimuli, participants were most likely to report the outermost flanker when they made an error. But for letters in the left visual field, they were more likely to report the inner flanker than the outer flanker (and less likely to make substitution errors overall). We propose that for *all* stimulus types the integration zones extend farther into the periphery than towards the fovea. But for letters, participants have a different strategy for reporting the central letter when uncertain, avoiding the identity of the leftmost letter that they can clearly identify.

The influences of reading experience and cerebral lateralization

Our interpretation has some attributes in common with the conclusions of an elegant study by Winsler & Luck (2025). In a sample of 250 participants, they found that crowding distances in the right visual field predicted individual differences in spelling ability, a proxy for reading expertise. Crowding in the left visual field did not correlate with spelling ability as strongly. These results are consistent with our hypothesis: reading experience reduces crowding for letters in the right visual field. (The data are also consistent with other hypotheses with different directions of causality).

However, there are some differences between studies: primarily, Winsler & Luck also found reduced crowding in the right visual field for non-letters (specifically, Gabor patches). They proposed that this stimulus-general hemifield asymmetry is caused by experience reading

English, which typically requires attending to the right parafovea. They therefore predict a reversed hemifield asymmetry for readers of a right-to-left orthography. That does not seem to hold, however; Hebrew readers demonstrate the same right visual field advantage for crowded Hebrew letters (Shechter et al., 2024). Moreover, this hypothesis makes two predictions: (1) Literacy skills should covary with the magnitude of the hemifield asymmetry of crowding for non-letters. That has not been tested. (2) Across individuals, the hemifield asymmetry for letters should correlate with the asymmetry for non-letters. In our exploratory analysis of individual differences (which is likely underpowered), we found only that correlations of the asymmetries between letters and non-letters were very weak (e.g., r=0.19 for letters vs. boxes, as compared to r=0.59 for pseudo-letters vs. boxes).

Given evidence that the right visual field advantages for both crowded letters and whole word recognition are common across languages and writing systems (see the Introduction), we prefer the hypothesis that they are driven by the cerebral lateralization of language function. A right visual field advantage for letter recognition is present as soon as children learn to read, but not before (Davidoff & Done, 1984; Jablonowska & Budohoska, 1976); see also (Ducrot & Grainger, 2025).

We are not sure, however, that the right visual field advantage for crowded letters can be equated to the right visual field advantage for whole words. The former likely contributes to the latter, but there seems to be an additional factor that accounts for the asymmetry for words. When letters are stacked vertically rather than horizontally, the asymmetry for letters is absent (Kurzawski et al., 2023), but the asymmetry for words persists (Barton et al., 1965; Young & Ellis, 1985). Moreover, in some cases, the right field advantage for letters is stronger for real words than non-word letter strings (Cutler et al., 2024).

Alternative explanation: a compensatory mechanism downstream of crowding

There is an alternative to our modified receptive field hypothesis: crowding operates in the same way for all stimuli and in both hemifields, at a relatively early level when features of multiple objects get integrated or pooled within constant zones before each object is identified by category-specific mechanisms. However, for letters, there is a downstream compensatory mechanism that improves accuracy specifically for letters in the right visual field. Specifically, readers may have learned what crowded letters *look like* when degraded by flankers in the right parafovea. The stronger learning for the right parafovea is due to the left-to-right direction in which English is read.

This is a reasonable explanation, but we have two reservations about it: (1) The appearance of a crowded letter likely depends on the specific shapes of its flankers. This might predict that the hemifield asymmetry is present only for common words or trigrams, but we used uncommon non-word trigrams. We also found a hemifield asymmetry when target letters

were flanked by unfamiliar pseudo-letters, which could not be readily transformed into a higher-level code (e.g., conceptual names or phonemes). (2) This alternate hypothesis predicts the reverse asymmetry in readers of Hebrew, who typically attend to letters in the left parafovea. But as noted above, there is also a right visual field advantage for crowding of Hebrew letters (Shechter et al., 2024)

Implications for models of crowding

Any complete model of crowding must explain the letter-specific hemifield asymmetry, just as it must explain the upper-vs-lower meridian asymmetry and the radial-tangential asymmetry. It should also be able to predict crowding distance thresholds for all types of stimuli. As noted above, theories of crowding differ in terms of whether they assume a single stage of feature integration that applies to all stimuli in a similar way.

There are other lines of evidence that crowding is not domain-general: crowding has different effects on color perception and motion perception (Greenwood & Parsons, 2020). Also, for letters and digits, the degree of crowding is modulated by whether a character's flankers are in the same category or not, and whether the flankers are meaningful or unfamiliar (Reuther & Chakravarthi, 2014)

One theory that accounts for such results is that crowding occurs at many stages of the visual hierarchy, including in category-specific systems (Manassi & Whitney, 2018). The "hierarchical sparse selection" framework attributes crowding to a readout mechanism that selects stimulus information for conscious access from a small number of neurons tuned to the specific category of the stimulus (Chaney et al., 2014). According to its authors, this model makes two predictions (among others), which our data confirm:

(1) "Critical spacing of crowding is different for different stimulus categories (e.g., gratings, faces, bodies, objects, etc.) because crowding is a function of receptive field size within the cortical map in which the stimulus is represented." Our data are consistent with this prediction (contrary to the claim by Wallace & Tjan, 2011).
(2) "With extensive experience viewing a particular stimulus category at a particular position in the visual field, it may be possible to reduce crowding through training… However, such training should not transfer to other sufficiently different stimulus categories even at the same spatial location because crowding depends on connections to the particular map that the stimuli are represented in." Our data are consistent with this prediction: the right visual field advantage is specific to letters, likely due to extensive training to read.

Our result therefore poses a challenge to theories of crowding that assume a single stage of feature integration applies to all objects. Those theories may need to be elaborated to

explain a specific reduction in crowding distances for one category of stimulus in one half of the visual field.

Limitations

One limitation of this study is that we examined crowding distances at only one eccentricity, 4º. Other studies have learned much about the mechanisms of crowding by testing at a wide range of eccentricities. However, Winsler & Luck (2025) found strong asymmetries for letters at 6º, 4º and 2º, and they found that crowding thresholds at 2 – 6º in the right visual field predicted individual differences in spelling ability. Thus, we are confident that we chose visual field positions that are generalizable and relevant to naturalistic tasks.

We also only positioned our flankers horizontally, that is, radially with respect to fixation. The hemifield asymmetry for letters is weak or absent when the flankers are oriented tangentially above/below the target (Kurzawski et al., 2023). Moreover, the general advantage for crowded letters, compared to symbols, seems to be specific to horizontally-arranged strings, across the visual field (Vejnović & Zdravković, 2015). Thus, the unique patterns of crowding we observed for letters may be specific to letters arranged in the way they are usually read, due to perceptual learning over the course of literacy acquisition (Winsler & Luck, 2025).

We look forward to future studies that test a wider range of stimulus conditions and that examine correlations across conditions with larger sample sizes. Our exploratory analysis of individual differences suggested hemifield-specific crowding that partially generalizes across stimulus types, but our study was underpowered to detect subtle differences in correlation coefficients.

Conclusion

Crowding affects the identification of letters differently than other stimulus types with similar visual features. Crowding distances are overall lower for letters, meaning that letters can be identified when closer together than other stimuli can be. Moreover, letters enjoy a specific advantage in the right visual field, where they crowd each other even less. This hemifield asymmetry is likely a result of perceptual learning that modified visual processing for a specific category of shapes. We hypothesis that it is driven reading experience and shaped by the typical (in most people) lateralization of language functions to the left cerebral hemisphere, which preferentially processes information in the right visual field.

Therefore, the mechanisms of crowding may not be the same for all categories of stimuli. Ironically, although the study of crowding began with letters, letters are special because they are not components of natural scenes. To read, it is not helpful for the visual system to extract summary statistics about letters on a page. Letters need to be identified individually

and as parts of whole words. These unique demands of reading sharpen the spatial tuning of mechanisms that identify crowded letters, especially in the right visual field.

Acknowledgements: This project was supported by funding from the National Eye Institute (grant R00 EY-029366). The authors have no conflicts of interest to declare.

Data availability: The raw data and analysis code will be shared publicly on Zenodo upon publication.

References

Adamson, M. M., & Hellige, J. B. (2006). Hemispheric differences for identification of words and nonwords in Urdu-English bilinguals. *Neuropsychology*, *20*(2), 232–248. https://doi.org/10.1037/0894-4105.20.2.232

Arguin, M., Joanette, Y., & Cavanagh, P. (1990). Comparing the cerebral hemispheres on the speed of spatial shifts of visual attention: Evidence from serial search. *Neuropsychologia*, *28*(7), 733–736. https://doi.org/10.1016/0028-3932(90)90128-B

Banks, W. P., Bachrach, K. M., & Larson, D. W. (1977). The asymmetry of lateral interference in visual letter identification. *Perception & Psychophysics*, *22*(3), 232–240. https://doi.org/10.3758/BF03199684

Barton, M. I., Goodglass, H., & D Amnon Shai, A. N. (1965). Differential recognition of tachistoscopically presented English and Hebrew words in right and left visual fields. *Perceptual and Motor Skills*, *21*(21), 431–437.

Behrmann, M., & Plaut, D. C. (2020). Hemispheric Organization for Visual Object Recognition : A Theoretical Account and Empirical Evidence. *Perception*, (August 2019), 030100661989904. https://doi.org/10.1177/0301006619899049

Benjamini, Y., & Hochberg, Y. (1995). Controlling the False Discovery Rate: A Practical and Powerful Approach to Multiple Testing. *Journal of the Royal Statistical Society. Series B (Methodological)*, *57*(1), 289–300. http://www.jstor.org/stable/10.2307/2346101

Bertoni, S., Franceschini, S., Ronconi, L., Gori, S., & Facoetti, A. (2019). Is excessive visual crowding causally linked to developmental dyslexia? *Neuropsychologia*, *130*(May), 107–117. https://doi.org/10.1016/j.neuropsychologia.2019.04.018

Bouma, H. (1970). Interaction effects in parafoveal letter recognition. *Nature*, *226*, 177–178. http://adsabs.harvard.edu/abs/1970Natur.226..177B

Bouma, H. (1973). Visual interference in the parafoveal recognition of initial and final letters of words. *Vision Research*, *13*(4), 767–782. https://doi.org/10.1016/0042-6989(73)90041-2

Brainard, D. H. (1997). The psychophysics toolbox. *Spatial Vision*, *10*, 443–446.

Brederoo, S. G., Nieuwenstein, M. R., Cornelissen, F. W., & Lorist, M. M. (2019). Reproducibility of visual-field asymmetries: Nine replication studies investigating lateralization of visual information processing. *Cortex*, *111*, 100–126. https://doi.org/10.1016/j.cortex.2018.10.021

Brederoo, S. G., Nieuwenstein, M. R., Lorist, M. M., & Cornelissen, F. W. (2017). Hemispheric specialization for global and local processing: A direct comparison of linguistic and non-linguistic stimuli. *Brain and Cognition*, *119*, 10–16. https://doi.org/10.1016/j.bandc.2017.09.005

Callens, M., Whitney, C., Tops, W., & Brysbaert, M. (2013). No deficiency in left-to-right processing of words in dyslexia but evidence for enhanced visual crowding. *Quarterly Journal of Experimental Psychology*, *66*(9), 1803–1817. https://doi.org/10.1080/17470218.2013.766898

Carlei, C., & Kerzel, D. (2018). Stronger interference from distractors in the right hemifield during visual search. *Laterality*, *23*(2), 152–165. https://doi.org/10.1080/1357650X.2017.1327539

Castet, E., Descamps, M., Denis-Noël, A., & Colé, P. (2017). Letter and symbol identification: No evidence for letter-specific crowding mechanisms. *Journal of Vision*, *17*(11), 2. https://doi.org/10.1167/17.11.2

Chanceaux, M., & Grainger, J. (2012). Serial position effects in the identification of letters, digits, symbols, and shapes in peripheral vision. *Acta Psychologica*, *141*(2), 149–158. https://doi.org/10.1016/j.actpsy.2012.08.001

Chanceaux, M., Mathôt, S., & Grainger, J. (2013). Flank to the left, flank to the right: Testing the modified receptive field hypothesis of letter-specific crowding. *Journal of Cognitive Psychology*, *25*(6), 774–780. https://doi.org/10.1080/20445911.2013.823436

Chaney, W., Fischer, J., & Whitney, D. (2014). The hierarchical sparse selection model of visual crowding. *Frontiers in Integrative Neuroscience*, *8*(SEP). https://doi.org/10.3389/fnint.2014.00073

Chang, C. H. C., Pallier, C., Wu, D. H., Nakamura, K., Jobert, A., Kuo, W. J., & Dehaene, S. (2015). Adaptation of the human visual system to the statistics of letters and line configurations. *NeuroImage*, *120*, 428–440. https://doi.org/10.1016/j.neuroimage.2015.07.028

Coates, D. R., Ludowici, C. J. H., & Chung, S. T. L. (2021). The generality of the critical spacing for crowded optotypes: From Bouma to the 21st century. *Journal of Vision*, *21*(11), 1–22. https://doi.org/10.1167/jov.21.11.18

Crovitz, H. F., & Schiffman, H. R. (1965). Visual field and the letter span. *Journal of Experimental Psychology*, *70*(2), 218–223.

Cutler, J., Bodet, A., Rivest, J., & Cavanagh, P. (2024). The word superiority effect overcomes crowding. *Vision Research*, *222*(May). https://doi.org/10.1016/j.visres.2024.108436

Davidoff, J. B., & Done, D. J. (1984). A longitudinal study of the development of visual field advantage for letter matching. *Neuropsychologia*, *22*(3), 311–318. https://doi.org/10.1016/0028-3932(84)90078-2

Dehaene, S., Cohen, L., Morais, J., & Kolinsky, R. (2015). Illiterate to literate: behavioural and cerebral changes induced by reading acquisition. *Nature Reviews Neuroscience*, *16*(4), 234–244. https://doi.org/10.1038/nrn3924

Dehaene, S., Pegado, F., Braga, L. W., Ventura, P., Nunes Filho, G., Jobert, A., Dehaene-Lambertz, G., Kolinsky, R., Morais, J., & Cohen, L. (2010). How learning to read changes the cortical networks for vision and language. *Science*, *330*(6009), 1359–1364. https://doi.org/10.1126/science.1194140

Dehaene-Lambertz, G., Monzalvo, K., & Dehaene, S. (2018). The emergence of the visual word form: Longitudinal evolution of category-specific ventral visual areas during reading acquisition. *PLOS Biology*, *16*(3), e2004103. https://doi.org/10.1371/journal.pbio.2004103

Ducrot, S., & Grainger, J. (2007). Deployment of spatial attention to words in central and peripheral vision. *Perception & Psychophysics*, *69*(4), 578–590. https://doi.org/10.3758/BF03193915

Ducrot, S., & Grainger, J. (2025). The development of letter representations in preschool children is affected by visuomotor integration skills and visual field asymmetries. *Journal of Experimental Child Psychology*, *257*(December 2024), 106277. https://doi.org/10.1016/j.jecp.2025.106277

Dundas, E. M., Plaut, D. C., & Behrmann, M. (2013). The joint development of hemispheric lateralization for words and faces. *Journal of Experimental Psychology: General*, *142*(2), 348–358. https://doi.org/10.1037/a0029503

Ehlers, H. (1936). The Movements of the Eyes During Reading. *Acta Ophthalmologica*, *14*(1–2), 56–63. https://doi.org/10.1111/j.1755-3768.1936.tb07306.x

Ehlers, H. (1953). Clinical testing of visual acuity. *AMA Archives of Ophthalmology*, *49*(4), 431–434.

Eriksen, B. A., & Eriksen, C. W. (1974). Effects of noise letters upon the identification of a target letter in a nonsearch task. In *Perception & Psychophysics* (Vol. 16, Number 1, pp. 143–149). https://doi.org/10.3758/BF03203267

Estes, W. K., Allmeyer, D. H., & Reder, S. M. (1976). Serial position functions for letter identification at brief and extended exposure durations. In *Perception & Psychophysics* (Vol. 19, Number 1).

Evert, D. L., McGlinchey-Berroth, R., Verfaellie, M., & Milberg, W. P. (2003). Hemispheric asymmetries for selective attention apparent only with increased task demands in healthy participants. *Brain and Cognition*, *53*(1), 34–41. https://doi.org/10.1016/S0278-2626(03)00207-0

Faust, M., Kravetz, S., & Babkoff, H. (1993). Hemispheric specialization or reading habits: Evidence from lexical decision research with hebrew words and sentences. *Brain and Language*, *44*(3), 254–263. https://doi.org/10.1006/brln.1993.1017

Freeman, J., Chakravarthi, R., & Pelli, D. G. (2012). Substitution and pooling in crowding. *Attention, Perception, and Psychophysics*, *74*(2), 379–396. https://doi.org/10.3758/s13414-011-0229-0

Frömer, R., Dimigen, O., Niefind, F., Krause, N., Kliegl, R., & Sommer, W. (2015). Are individual differences in reading speed related to extrafoveal visual acuity and crowding? *PLoS ONE*, *10*(3), 1–18. https://doi.org/10.1371/journal.pone.0121986

Gori, S., & Facoetti, A. (2015). How the visual aspects can be crucial in reading acquisition: The intriguing case of crowding and developmental dyslexia. *Journal of Vision*, *15*(1), 1–20. https://doi.org/10.1167/15.1.8

Grainger, J., Dufau, S., & Ziegler, J. C. (2016). A Vision of Reading. *Trends in Cognitive Sciences*, *20*(3), 171–179. https://doi.org/10.1016/j.tics.2015.12.008

Grainger, J., Tydgat, I., & Isselé, J. (2010). Crowding Affects Letters and Symbols Differently. *Journal of Experimental Psychology: Human Perception and Performance*, *36*(3), 673–688. https://doi.org/10.1037/a0016888

Greenwood, J. A., & Parsons, M. J. (2020). Dissociable effects of visual crowding on the perception of color and motion. *Proceedings of the National Academy of Sciences*, *117*(14), 8196–8202. https://doi.org/10.1073/pnas.1909011117

Greenwood, J. A., Szinte, M., Sayim, B., & Cavanagh, P. (2017). Variations in crowding, saccadic precision, and spatial localization reveal the shared topology of spatial vision. *Proceedings of the National Academy of Sciences of the United States of America*, *114*(17), E3573–E3582. https://doi.org/10.1073/pnas.1615504114

Harrison, W. J., Mattingley, J. B., & Remington, R. W. (2013). Eye movement targets are released from visual crowding. *Journal of Neuroscience*, *33*(7), 2927–2933. https://doi.org/10.1523/JNEUROSCI.4172-12.2013

Herzog, M. H., & Manassi, M. (2015). Uncorking the bottleneck of crowding: A fresh look at object recognition. *Current Opinion in Behavioral Sciences*, *1*, 86–93. https://doi.org/10.1016/j.cobeha.2014.10.006

Himmelberg, M. M., Winawer, J., & Carrasco, M. (2023). Polar angle asymmetries in visual perception and neural architecture. *Trends in Neurosciences*, *46*(6), 445–458. https://doi.org/10.1016/j.tins.2023.03.006

Hines, D. (1978). Visual information processing in the left and right hemispheres. *Neuropsychologia*, *16*(5), 593–600. https://doi.org/10.1016/0028-3932(78)90087-8

Huckauf, A., & Heller, D. (2002). What various kinds of errors tell us about lateral masking effects. *Visual Cognition*, *9*(7), 889–910. https://doi.org/10.1080/13506280143000548A

Huckauf, A., Heller, D., & Nazir, T. A. (1999). Lateral masking: Limitations of the feature interaction account. *Perception & Psychophysics*, *61*(1), 177–189.

Hussain, Z., Webb, B. S., Astle, A. T., & McGraw, P. V. (2012). Perceptual learning reduces crowding in amblyopia and in the normal periphery. *Journal of Neuroscience*, *32*(2), 474–480. https://doi.org/10.1523/JNEUROSCI.3845-11.2012

Ibrahim, R., & Eviatar, Z. (2009). Language Status and Hemispheric Involvement in Reading: Evidence From Trilingual Arabic Speakers Tested in Arabic, Hebrew, and English. *Neuropsychology*, *23*(2), 240–254. https://doi.org/10.1037/a0014193

Ibrahim, R., & Eviatar, Z. (2012). The contribution of the two hemispheres to lexical decision in different languages. *Behavioral and Brain Functions*, *8*, 1–7. https://doi.org/10.1186/1744-9081-8-3

Jablonowska, K., & Budohoska, W. (1976). Hemispheric differences in the visual analysis of the verbal and non-verbal material in children. *Acta Neurobiologiae Experimentalis*, *36*(6), 693–701.

Joo, S. J., White, A. L., Strodtman, D. J., & Yeatman, J. D. (2018). Optimizing text for an individual's visual system: The contribution of crowding to reading difficulties. *Cortex*, *103*, 291–301. https://doi.org/10.1016/j.cortex.2018.03.013

Kewan-Khalayly, B., Migó, M., & Yashar, A. (2022). Transient attention equally reduces visual crowding in radial and tangential axes. *Journal of Vision*, *22*(9), 1–9. https://doi.org/10.1167/jov.22.9.3

Kooi, F. L., Toet, A., Tripathy, S. P., & Levi, D. M. (1994). The effect of similarity and duration on spatial interaction in peripheral vision. *Spatial Vision*, *8*(2), 255–279. https://doi.org/10.1163/156856894X00350

Kurzawski, J. W., Burchell, A., Thapa, D., Winawer, J., Majaj, N. J., & Pelli, D. G. (2023). The Bouma law accounts for crowding in 50 observers. *Journal of Vision*, *23*(8), 1–34. https://doi.org/10.1167/jov.23.8.6

Kurzawski, J. W., Qiu, B. S., Majaj, N. J., Benson, N. C., Pelli, D. G., & Winawer, J. (2025). Human V4 size predicts crowding distance. *Nature Communications*, *16*(1), 1–11. https://doi.org/10.1038/s41467-025-59101-w

Leehey, S. C., & Cahn, A. (1979). Lateral asymmetries in the recognition of words, familiar faces and unfamiliar faces. *Neuropsychologia*, *17*(6), 619–628. https://doi.org/10.1016/0028-3932(79)90036-8

Legge, G. E., Cheung, S.-H. S. H., Yu, D., Chung, S. T. L., Lee, H.-W. H. W., & Owens, D. P. (2007). The case for the visual span as a sensory bottleneck in reading. *Journal of Vision*, *7*(2), 1–15. https://doi.org/10.1167/7.2.9.Introduction

Legge, G. E., Mansfield, J. S., & Chung, S. T. L. (2001). Psychophysics of reading XX. Linking letter recognition to reading speed in central and peripheral vision. *Vision Research*, *41*, 725–743.

Levi, D. M. (2008). Crowding-An essential bottleneck for object recognition: A mini-review. *Vision Research*, *48*(5), 635–654. https://doi.org/10.1016/j.visres.2007.12.009

Liu, R., Patel, B. N., & Kwon, M. Y. (2017). Age-related changes in crowding and reading speed. *Scientific Reports*, *7*(1), 1–10. https://doi.org/10.1038/s41598-017-08652-0

Mackworth, N. H. (1965). Visual noise causes tunnel vision. *Psychonomic Science*, *3*(1–12), 67–68. https://doi.org/10.3758/bf03343023

Manassi, M., France, B. S., & Herzog, M. H. (2012). Grouping, pooling, and when bigger is better in visual crowding. *Journal of Vision*, *12*(10), 1–14. https://doi.org/10.1167/12.10.13

Manassi, M., & Whitney, D. (2018). Multi-level Crowding and the Paradox of Object Recognition in Clutter. *Current Biology*, *28*(3), R127–R133. https://doi.org/10.1016/j.cub.2017.12.051

Martelli, M., Di Filippo, G., Spinelli, D., Zoccolotti, P., Filippo, G. Di, Spinelli, D., & Zoccolotti, P. (2009). Crowding, reading, and developmental dyslexia. *Journal of Vision*, *9*(4), 1–18. https://doi.org/10.1167/9.4.14.Introduction

Martelli, M., Majaj, N. J., & Pelli, D. G. (2005). Are faces processed like words? A diagnostic test for recognition by parts. *Journal of Vision*, *5*(1), 58–70. https://doi.org/10.1167/5.1.6

Meyyappan, S., Rajan, A., Mangun, G. R., & Ding, M. (2023). Top-down control of the left visual field bias in cued visual spatial attention. *Cerebral Cortex*, *33*(9), 5097–5107. https://doi.org/10.1093/cercor/bhac402

Michael, G. A., & Ojéda, N. (2005). Visual field asymmetries in selective attention: Evidence from a modified search paradigm. *Neuroscience Letters*, *388*(2), 65–70. https://doi.org/10.1016/j.neulet.2005.06.027

Mishkin, M., & Forgays, D. G. (1952). Word recognition as a function of retinal locus. *Journal of Experimental Psychology*, *43*(1), 43–48. https://doi.org/10.1037/h0061361

Nordt, M., Gomez, J., Natu, V. S., Rezai, A. A., Finzi, D., Kular, H., & Grill-Spector, K. (2021). Cortical recycling in high-level visual cortex during childhood development. *Nature Human Behaviour*, *5*, 1686–1697. https://doi.org/10.1038/s41562-021-01141-5

Ossowski, A., & Behrmann, M. (2015). Left hemisphere specialization for word reading potentially causes, rather than results from, a left lateralized bias for high spatial frequency visual information. *Cortex*, *72*, 27–39. https://doi.org/10.1016/j.cortex.2014.12.013

Parkes, L., Lund, J., Angelucci, A., Solomon, J. A., & Morgan, M. (2001). Compulsory averaging of crowded orientation signals in human vision. *Nature Neuroscience*, *4*(7), 739–744. https://doi.org/10.1038/89532

Pegado, F., Comerlato, E., Ventura, F., Jobert, A., Nakamura, K., Buiatti, M., Ventura, P., Dehaene-Lambertz, G., Kolinsky, R., Morais, J., Braga, L. W., Cohen, L., & Dehaene, S. (2014). Timing the impact of literacy on visual processing. *Proceedings of the National Academy of Sciences*, *111*(49), E5233–E5242. https://doi.org/10.1073/pnas.1417347111

Pelli, D. G. (1997). The VideoToolbox software for visual psychophysics: Transforming numbers into movies. *Spatial Vision*, *10*, 437–442.

Pelli, D. G., Palomares, M., & Majaj, N. J. (2004). Crowding is unlike ordinary masking: Distinguishing feature integration from detection. *Journal of Vision*, *4*(12), 1136–1169. https://doi.org/10.1167/4.12.12

Pelli, D. G., & Tillman, K. A. (2008). The uncrowded window of object recognition. *Nature Neuroscience*, *11*(10), 1129–1135. https://doi.org/10.1038/nn.2187

Pelli, D. G., Tillman, K. A., Freeman, J., Su, M., Berger, T. D., & Majaj, N. J. (2007). Crowding and eccentricity determine reading rate. *Journal of Vision*, *7*(2), 1–36. https://doi.org/10.1167/7.2.20.Modeling

Peyrin, C., Chauvin, A., Chokron, S., & Marendaz, C. (2003). Hemispheric specialization for spatial frequency processing in the analysis of natural scenes. *Brain and Cognition*, *53*(2), 278–282. https://doi.org/10.1016/S0278-2626(03)00126-X

Prins, N. (2012). The psychometric function: The lapse rate revisited. *Journal of Vision*, *12*, 1–16. https://doi.org/10.1167/12.6.25.Introduction

Prins, N., & Kingdom, F. A. A. (2018). Applying the model-comparison approach to test specific research hypotheses in psychophysical research using the Palamedes toolbox. *Frontiers in Psychology*, *9*(JUL). https://doi.org/10.3389/FPSYG.2018.01250/FULL

Ramamurthy, M., White, A. L., Chou, C., & Yeatman, J. D. (2021). Spatial attention in encoding letter combinations. *Scientific Reports*, *11*(1), 1–12. https://doi.org/10.1038/s41598-021-03558-4

Ransley, K., Goodbourn, P. T., Nguyen, E. H. L., Moustafa, A. A., & Alex, O. (2018). Reading Direction Influences Lateral Biases in Letter Processing. *Journal of Experimental*

Psychology: Learning, Memory, and Cognition, *44*(10), 1678–1686. https://doi.org/http://dx.doi.org/10.1037/xlm0000540

Reuther, J., & Chakravarthi, R. (2014). Categorical membership modulates crowding: Evidence from characters. *Journal of Vision*, *14*(6). https://doi.org/10.1167/14.6.5

Rosenholtz, R., Yu, D., & Keshvari, S. (2019). Challenges to pooling models of crowding: Implications for visual mechanisms. *Journal of Vision*, *19*(7), 15. https://doi.org/10.1167/jov.19.7.15

Sergent, J. (1982). The cerebral balance of power: Confrontation or cooperation? *Journal of Experimental Psychology: Human Perception and Performance*, *8*(2), 253–272. https://doi.org/10.1037/0096-1523.8.2.253

Shechter, A., Medina, S., Share, D. L., & Yashar, A. (2024). Language-universal and script-specific factors in the recognition of letters in visual crowding: The effects of lexicality, hemifield, and transitional probabilities in a right-to-left script. *Cortex*, *171*, 319–329. https://doi.org/10.1016/j.cortex.2023.10.021

Shechter, A., & Yashar, A. (2021). Mixture model investigation of the inner–outer asymmetry in visual crowding reveals a heavier weight towards the visual periphery. *Scientific Reports*, *11*(1). https://doi.org/10.1038/s41598-021-81533-9

Siéroff, E., & Haehnel-Benoliel, N. (2015). Environmental script affects lateral asymmetry of word recognition: A study of French–Hebrew bilinguals tested in Israel and in France. *Laterality*, *20*(4), 389–417. https://doi.org/10.1080/1357650X.2014.988220

Song, S., Levi, D. M., & Pelli, D. G. (2014). A double dissociation of the acuity and crowding limits to letter identification, and the promise of improved visual screening. *Journal of Vision*, *14*(5), 3–3. https://doi.org/10.1167/14.5.3

Strasburger, H. (2020). Seven Myths on Crowding and Peripheral Vision. *I-Perception*, *11*(3). https://doi.org/10.1177/2041669520913052

Strasburger, H., & Malania, M. (2013). Source confusion is a major cause of crowding. *Journal of Vision*, *13*(1), 24–24. https://doi.org/10.1167/13.1.24

Tadros, K., Dupuis-Roy, N., Fiset, D., Arguin, M., & Gosselin, F. (2013). Reading laterally: The cerebral hemispheric use of spatial frequencies in visual word recognition. *Journal of Vision*, *13*(1). https://doi.org/10.1167/13.1.4

Toet, A., & Levi, D. M. (1992). The two-dimensional shape of spatial interaction zones in the parafovea. *Vision Research*, *32*(7), 1349–1357. https://doi.org/10.1016/0042-6989(92)90227-A

Torgesen, J., Rashotte, C., & Wagner, R. (1999). TOWRE-2: Test of Word Reading Efficiency, 2nd Ed. In *Austin, TX: Pro-Ed*.

Tydgat, I., & Grainger, J. (2009). Serial Position Effects in the Identification of Letters, Digits, and Symbols. *Journal of Experimental Psychology: Human Perception and Performance*, *35*(2), 480–498. https://doi.org/10.1037/a0013027

Vejnović, D., & Zdravković, S. (2015). Side flankers produce less crowding, but only for letters. *Cognition*, *143*, 217–227. https://doi.org/10.1016/j.cognition.2015.07.003

Vidal, C., Content, A., & Chetail, F. (2017). BACS: The Brussels Artificial Character Sets for studies in cognitive psychology and neuroscience. *Behavior Research Methods*, *49*(6), 2093–2112. https://doi.org/10.3758/s13428-016-0844-8

Wallace, J. M., & Tjan, B. S. (2011). Object crowding. *Journal of Vision*, *11*(6), 1–17. https://doi.org/10.1167/11.6.19

White, A. L., Palmer, J., Boynton, G. M., & Yeatman, J. D. (2019). Parallel spatial channels converge at a bottleneck in anterior word-selective cortex. *Proceedings of the National Academy of Sciences*, *116*(24), 10087–10096. https://doi.org/10.1073/pnas.1822137116

White, M. J. (1969). Laterality differences in perception: A review. *Psychological Bulletin*, *72*(6), 387–405. https://doi.org/10.1037/h0028343

Whitney, D., & Levi, D. M. (2011). Visual crowding: A fundamental limit on conscious perception and object recognition. *Trends in Cognitive Sciences*, *15*(4), 160–168. https://doi.org/10.1016/j.tics.2011.02.005

Winsler, K., & Luck, S. J. (2025). A lifetime of reading experience facilitates the perception of crowded letters. *Journal of Memory and Language*, *145*. https://doi.org/10.1016/j.jml.2025.104689

Yashar, A., & Carrasco, M. (2024). When periphery rules : Enhanced sampling weights of the visual periphery in crowding across dimensions. *Psychonomic Bulletin & Review*, (0123456789). https://doi.org/10.3758/s13423-024-02580-7

Yashar, A., Chen, J., & Carrasco, M. (2015). Rapid and long-lasting reduction of crowding through training. *Journal of Vision*, *15*(10). https://doi.org/10.1167/15.10.15

Yeatman, J. D., & White, A. L. (2021). Reading: The Confluence of Vision and Language. *Annual Review of Vision Science*, *7*(1), 487–517. https://doi.org/10.1146/annurev-vision-093019-113509

Yeshurun, Y., & Rashal, E. (2010). Precueing attention to the target location diminishes crowding and reduces the critical distance. *Journal of Vision*, *10*(10). https://doi.org/10.1167/10.10.16

Young, A. W., & Ellis, A. W. (1985). Different methods of lexical access for words presented in the left and right visual hemifields. *Brain and Language*, *24*, 326–358.

Supplemental Materials for:

"The right visual field advantage for crowding is specific to letters"

By Alex White, Nicole Oppenheimer & Anishka Yerabothu

Experiment S1: Uncrowded size thresholds

This is a companion experiment to Experiment 1 reported in the main text. Using similar stimuli, we measured size thresholds for uncrowded targets presented singly without flankers. This provides an interesting comparison to the thresholds measured in Experiment 1, which in the main text were reported in terms of the target-flanker distance thresholds. Here we report the same data but in terms of the target width (because the target-flanker distances and target widths were scaled together with a ratio of 1.25).

Methods

Participants: 15 female volunteers were recruited from the same population as in Experiment 1, with the same criteria and informed consent procedures. Their mean age was 21 years (ranging from 18 to 31 years). Their mean score on the TOWRE test was 108 (SEM = 4.15). One was left-handed, and 13 were native English speakers. Five of these participants also participated in Experiment 1, and one also participated in Experiment 2.

Stimulus presentation and procedures: All details of the stimuli and task were identical to Experiment 1 except for the following factors:

- Each target shape was presented alone without flankers. The staircase procedure adjusted the stimulus width to measure size thresholds (i.e., acuity limits).
- The stimulus duration was 150 ms rather than 200 ms.
- In the set of 8 letters, we included a "u" instead of a "v."
- There were no spatial cues (the green lines) that in Experiment 1 appeared on both sides before the stimulus, and on the target's side after the stimulus. Instead, each trial began with a 700 ms fixation interval, then the 150 ms stimulus presentation, and then a 600 ms delay before the response alternatives appeared below the fixation mark.
- Trials were run in blocks of 48, rather than 40. The entire experiment required 48 blocks, yielding on average 300 trials per psychometric function.

Results and Discussion

Figure S1 compares the unflanked (uncrowded) size thresholds in this experiment to the *flanked (crowded)* size thresholds in Experiment 1. These flanked size thresholds are equal to the *crowding distance thresholds* (plotted in the main text Figure 3) divided by 1.25,

because during the staircase procedure the spacing and individual item width were scaled together: spacing = 1.25*width.

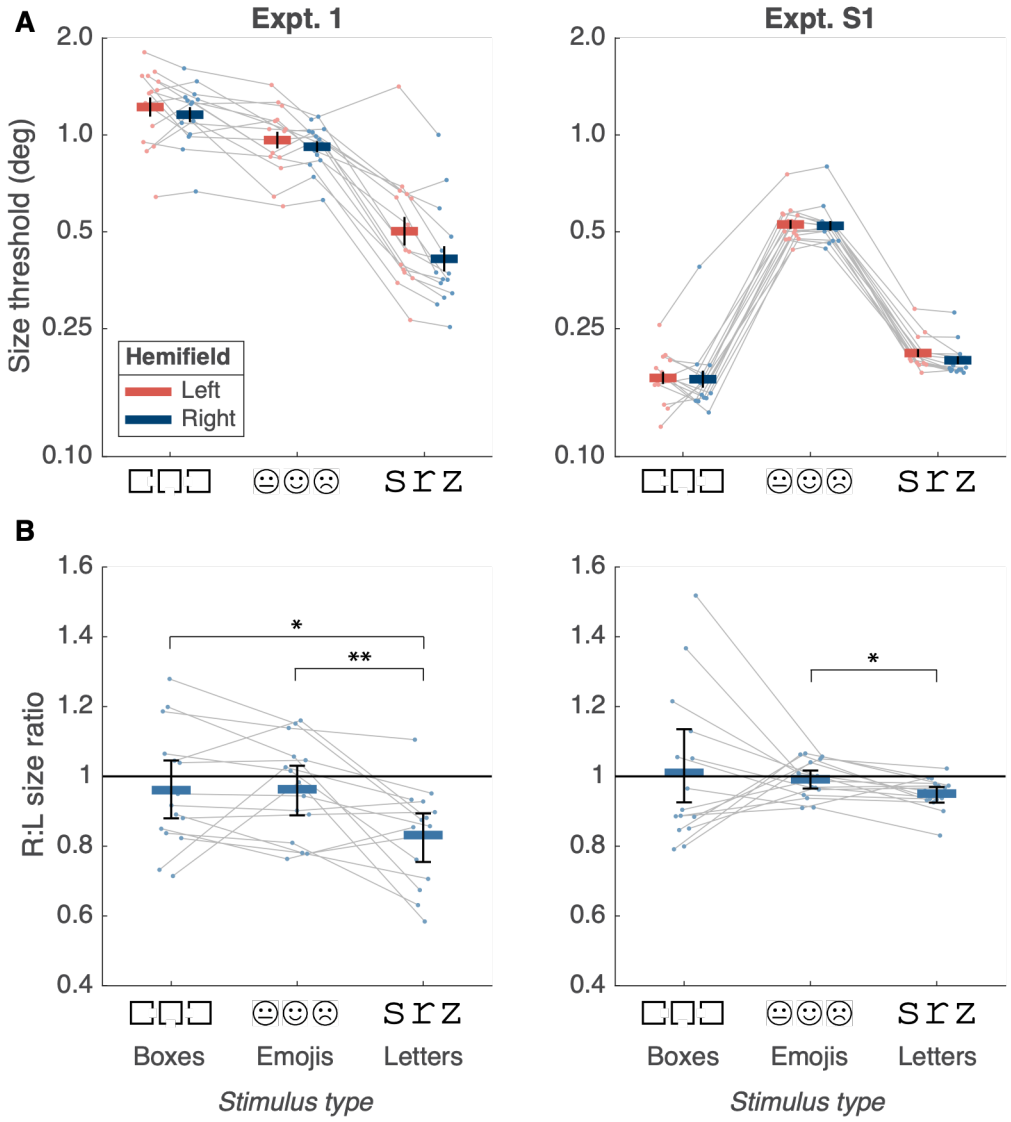

Figure S1: Comparing crowded size thresholds in Experiment 1 to uncrowded size thresholds in Experiment S1. (A) Top row: size (acuity) thresholds for the target shape's width in degrees, plotted on a $\log_{10}$ scale. The left panel is for Experiment 1 (crowded targets), showing the same thresholds as Figure 3A except scaled by a factor of 0.8 (to reflect the stimulus width at the spacing threshold). The right panel is for Experiment S1 (unflanked targets). Each point is one participant's threshold, and all points belonging to one participant are connected by a line. The darker horizontal lines are the across-participant means (red = target in left visual field; blue = target in right visual field) with error bars indicating +/- 1 SEM. **(B)** Bottom row: The hemifield asymmetries, expressed as the ratio of right:left size thresholds. Asterisks indicate significant pairwise differences in the hemifield asymmetry across stimulus types (* = p<0.05; **=p<0.01).

When the stimuli were crowded, boxes had the largest size thresholds of the three stimulus types **(Figure S1A, left)**, but when single targets were uncrowded, boxes had the smallest size thresholds (**Figure S1A, right)**. Emojis had intermediate crowded size thresholds (close to those for boxes), but by far the largest uncrowded size thresholds. Letters had the smallest crowded size thresholds, but letters had intermediate unflanked size thresholds (slightly but significantly larger than for boxes; $F(1,56)=35.8$, $p<10^{-6}$).

The different patterns of crowded vs. uncrowded size thresholds across stimulus types show that the perceptual limits imposed by crowding and acuity are distinct. It is surprising that the crowded thresholds were larger (worse) for boxes than emojis ($F(1,56)=82.6$, $p<10^{-11}$), but the uncrowded acuity thresholds were much *lower* (better) for the boxes than for emojis ($F(1,56)=1174$, $p<10^{-38}$). The acuity difference can be explained by the spatial scale of the image details required to distinguish each exemplar: the emojis are distinguished by the shape of the mouth, a small detail inside the shape which may itself be 'crowded' by the eyes and outline of the face. Thus, the uncrowded size thresholds must be rather large for emojis. The boxes are distinguished by a single gap that takes up 31% of its width, which can be localized even at very small box sizes, yielding tiny acuity thresholds (roughly 0.2 degrees for the box width on average). But when flanked by two other boxes with different orientations, the task becomes much more difficult and the whole trigram must be scaled by a factor of 6 on average to achieve the same box identification accuracy. In contrast, for emojis, the average crowded size threshold was only 1.9 times the average uncrowded size threshold. For letters, that ratio was 2.6.

			Mean size threshold (deg)		**Hemifield asymmetry (R:L ratio)**				
Targets	**Flankers**	**Expt.**	***Left***	***Right***	***Mean [SEM]***	***95% CI***	***t(14)***	***p***	***BF***
Boxes	Boxes	1	1.26	1.18	0.96 [0.04]	[0.88 1.05]	-0.90	0.384	0.372
Emojis	Emojis	1	0.99	0.93	0.96 [0.03]	[0.90 1.03]	-1.03	0.319	0.414
Letters	Letters	1	0.55	0.44	0.83 [0.03]	[0.76 0.90]	-4.73	0.0003	103.2
Boxes	–	S1	0.18	0.18	1.01 [0.05]	[0.93 1.15]	0.18	0.860	0.266
Emojis	–	S1	0.53	0.53	0.99 [0.01]	[0.96 1.02]	-0.59	0.562	0.306
Letters	–	S1	0.21	0.2	0.95 [0.01]	[0.92 0.97]	-4.13	0.0010	37.9

Table S1: Statistics on the mean size thresholds in the left and right visual fields, and the hemifield asymmetry expressed as the ratio of size thresholds in the right:left visual fields. The two comparisons with $p<0.05$ remain significant after false discovery rate correction (Benjamini & Hochberg, 1995) for the six tests in this table.

The disproportionately large effect on crowding for boxes could be because the four boxes were less distinct from each other than the four emojis or the eight letters. The four boxes are identical except rotated relative to each other, and therefore the target becomes more

confusable with its flankers. Letters, in contrast, are each unique shapes with a unique name, which may contribute to their smallest crowding thresholds overall.

We also analyzed hemifield asymmetries in these size thresholds. An LME model applied to individual uncrowded size thresholds (Expt. S1) yielded a main effect of stimulus type ($F(2,84) = 950.9$, $p<10^{-57}$), no main effect of hemifield ($F(1,84) = 1.70$, $p=0.20$), but a significant interaction between stimulus type and hemifield ($F(2,84) = 4.41$, $p=0.015$). The hemifield asymmetries (mean R:L ratios) with statistical test are listed in **Table S1**. The first three rows are for the crowded thresholds from Experiment 1, and the statistics are identical to what was reported in Table 1 in the main text. The last three rows are for the uncrowded size thresholds Experiment S1.

There was only a significant hemifield asymmetry (smaller acuity thresholds in the right visual field) for letters, and not for boxes or emojis. The asymmetry for letters was slight on average (5% lower thresholds in the right visual field than left) but only one out of the 15 participants had a reversed asymmetry. That asymmetry was significantly stronger for letters than emojis ($t(14)=2.83$, $p=0.013$, $BF=4.4$), but the difference between letters and boxes was not significant ($t(14)=1.06$, $p=0.31$, $BF=0.42$), primarily because of large individual variability in the asymmetry ratios for boxes.

The significant right field advantage in acuity thresholds for single uncrowded letters is somewhat surprising. For simple grating stimuli, acuity has been reported to be the same in the left and right visual fields (along the horizontal meridian), but much worse along the vertical meridian (Barbot et al., 2021). For letters, (Bouma & Legein, 1977) reported no hemifield asymmetry in accuracy for identifying isolated letters, but a right visual field advantage emerged for crowded letters in trigrams and whole word recognition.

In conclusion, the data in Experiment S1 with unflanked stimuli suggest that crowding and acuity limits are distinct, with stimulus-specific factors influencing each one. A stimulus-specific right visual field advantage also emerged for the size thresholds of uncrowded single letters. This would suggest that reading experience improves the spatial precision of encoding single letter shapes in the left cerebral hemisphere, in addition to reducing the impacts of crowding. However, we hesitate to draw strong conclusions from this one result, given the small effect size. We look forward to further investigations.

Correlations in crowding distances across individuals

In this section, we investigate individual differences in crowding distance thresholds. We evaluate how well an individual's threshold for one stimulus condition predicts their threshold for another condition. These correlations can reveal whether there are stimulus-specific, location-specific, or more generalized factors that vary across individuals and determine the severity of crowding. For each experiment we computed correlations coefficients for every pair of conditions defined by stimulus type (e.g., letters, boxes) and side (left vs. right hemifield). The resulting correlation matrices can be compared to the predictions of different models.

Crowding distance thresholds varied widely across individuals, with high test-retest reliability. For example, across the 30 participants in Experiments 1 and 2, crowding distances for letters in the right hemifield ranged from 0.31º to 1.25º. To measure the reliability of those individual differences, we calculated distance threshold for the odd- and even-numbered trials separately. The correlation coefficient between those two sets of thresholds was 0.87. To estimate what that correlation r^* would be if we had run the full experiment twice on all participants, we used the Spearman-Brown prediction formula;

$$r^* = \frac{2r}{1+r}$$

where r is the split-half correlation coefficient (0.87) for this example, and r^* is the "disattenuated" estimate of reliability. For letters on the right, r*= 0.93, which is high reliability. The reliabilities for all conditions are shown along the diagonals of the correlation matrices below.

Figure S2 shows correlations between crowding distance thresholds (on a $\log_{10}$ scale) for letters and boxes, integrating across the 30 participants in Experiments 1 and 2. We begin with this analysis because it has the most power. Panel A shows four example correlations with the thresholds for letters on the right side of fixation. The first plot is the reliability estimate just described, with thresholds for half the trials correlated with thresholds for the other half of trials. The subsequent plots in Figure S2A show correlations between thresholds for letters on the right (calculated with all trials) with thresholds for letters on the left (same stimulus type, different side), boxes on the right (different stimulus type, same side), and with boxes on the left (different stimulus type, different side).

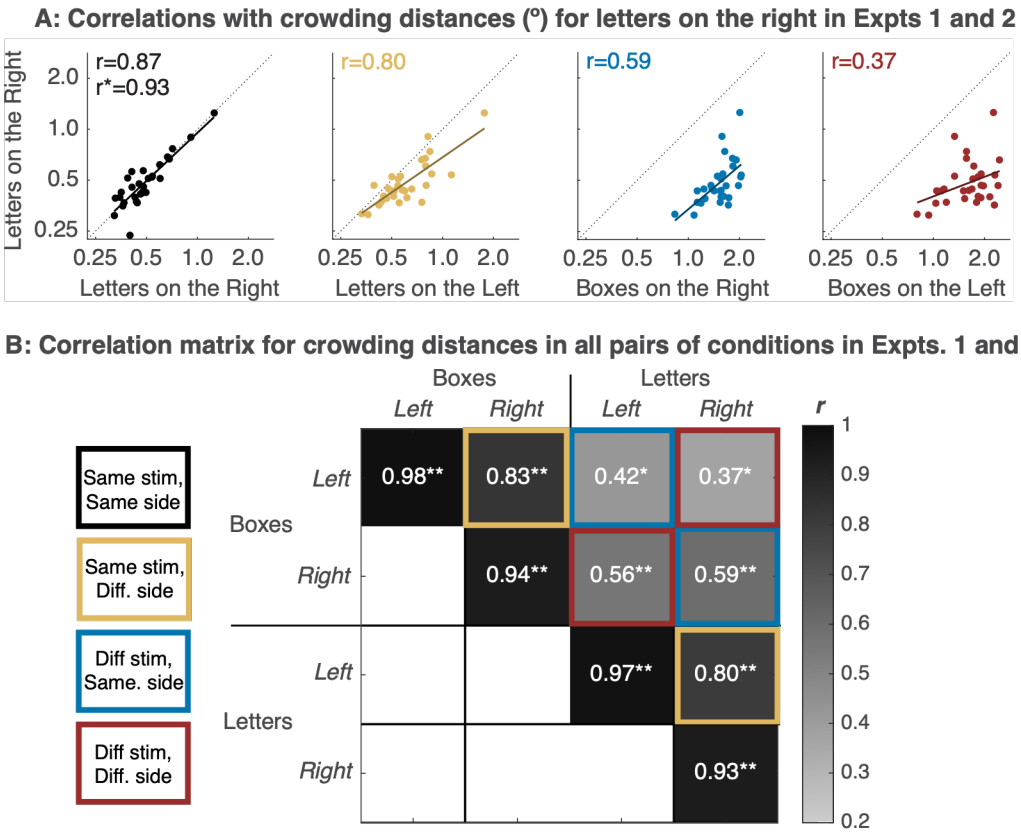

Figure S2: Correlations between crowding thresholds for the "letters" and "boxes" stimulus types, integrating across the 30 participants in Experiments 1 and 2. **(A)**: Four correlations with crowding distance thresholds for letters on the right. The units on the x- and y-axes are in degrees of visual angle on a $\log_{10}$ scale. The first panel is the split-half reliability for thresholds for letters on the right. The subsequent three panels are for letters on the right vs. other conditions (all trials included). **(B)** The full correlation matrix showing all 10 pairwise correlations between thresholds in Experiment 1 and 2. Asterisks indicate significant correlations (** p<0.01, * p<0.05). The grayscale shading within each square scales with the correlation coefficient r, as indicated by the color bar on the right. The values along the diagonal are the split-half reliability estimates, r* (see text).

Figure S2B show the full correlation matrix for letters and boxes in Experiments 1 and 2. The number in each square is the correlation coefficient for a particular pair of conditions, with asterisks indicating the statistical significance of that correlation. The grayscale lightness within each square corresponds to the correlation strength (darker = stronger). The outline of each square is colored according to the match between stimulus type and/or side in each condition, as indicated by the legend on the left. The values along the diagonal indicate test-retest reliabilities for each stimulus type and side (the values shown here are r* as explained above). Those are all quite high. Correlations are somewhat lower but still high for the same stimulus type but in the different side (yellow boxes, r=0.83 for

boxes and r=0.8 for letters). The correlations are lower when crossing stimulus types either in the same or different side, although there is a trend for higher correlations within the same side than across sides (blue vs red squares). Altogether, these data suggest a strong stimulus-specific mechanism that differs across individuals but generalizes across sides for each individual. There is also a hint of a hemifield-specific mechanism that differs across individuals and partly generalizes across stimulus types (e.g., r=0.59 for boxes on the right vs letters on the right).

It is also notable that there is a significant correlation for letters on the left vs boxes on the right (r=0.37, p=0.042). This suggests that crowding is partly determined by factors that vary across individuals but within an individual generalize across stimulus types and hemifields. Any factors that determine overall visual task performance could account for that correlation.

To better interpret the correlation matrix, we have four models that make predictions for how the correlation coefficients should vary when applied to thresholds for the same stimulus type, the same side, or neither. Each model makes a predicted correlation matrix, as shown in **Figure S3.**

*Model 1: Stimulus- and side-specific factors only, with some generalized variation in overall performance***.** Each individual's crowding thresholds are specific to a stimulus type and visual field location. Some factors that vary across individuals explain overall task performance and affect crowding thresholds generally, but equally so regardless of the stimulus type or side. This predicts that although there is high test-re-test reliability for the same stimulus type on the same side, but equally modest correlations for all other pairs of conditions.

Model 2: Side-specific factors that generalize across stimulus types. Crowding thresholds differ across sides (i.e., hemifields) and generalize across stimulus types within each side. This predicts that thresholds for each condition will correlate well with thresholds for different stimulus types measured on the same side (e.g., letters on the right vs. boxes on the right), but poorly with thresholds for the same stimulus type measured on the opposite side (e.g., letters on the right vs. letters on the left).

*Model 3: Stimulus-specific factors that generalize across sides***.** Crowding thresholds differ across stimulus types and generalize across sides for that stimulus type. This predicts that thresholds for each condition will correlate well with thresholds for the same stimulus type on the opposite side (e.g., letters on the right vs. letters on the left) but will correlate poorly with other stimulus types on the same side (e.g., letters on the right vs. boxes on the right).

Model 4: A mixture of stimulus-specific and side-specific factors. This model assumes a more complex correlation structure due to individual differences that partially generalize

across sides for a given stimulus type and partially generalize across stimulus types for a given side. This predicts the weakest correlations for different stimulus types in opposite sides (e.g., letters on the right vs. boxes on the left), and intermediate correlations for the same stimulus type measured in opposite sides or for different stimulus types measured on the same side.

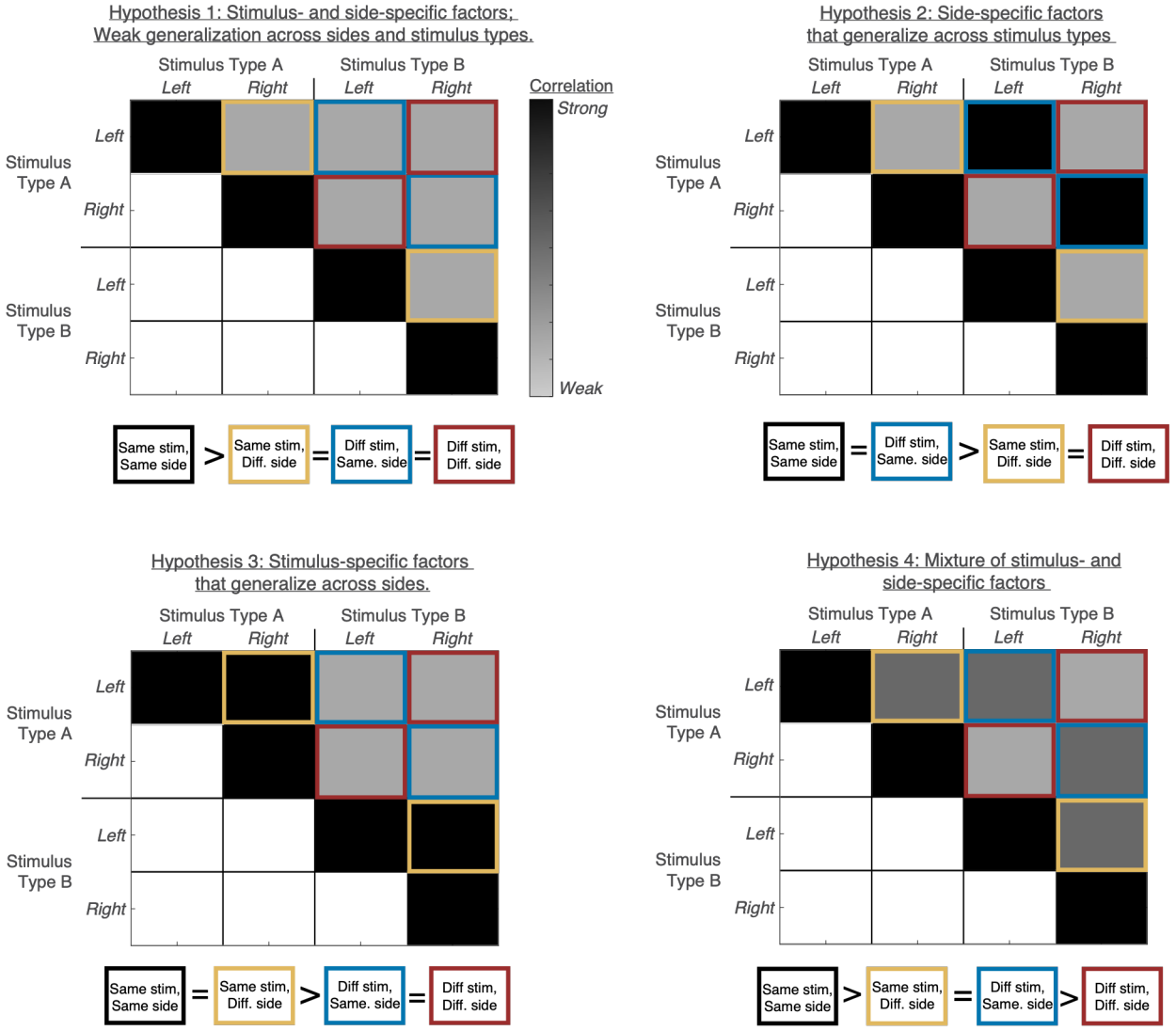

Figure S3: Correlation matrices predicted by four models, for correlations across crowding distances measured for two stimulus types and 2 sides.

Each model has a predicted correlation matrix, as shown in **Figure S3**. Each correlation takes one of three values: high (0.91), medium (0.73) or low (0.55). We chose these values to span the range of the average split-half reliabilities (0.91) to the average correlations across different stimulus types and different sides (0.55), with the medium level mid-way between.

For all three experiments (in addition to the data for boxes and letters integrated across Experiments 1 and 2), we compared the measured correlation matrix against the predicted correlation matrix for each model. To do so we simply transformed both matrices into vectors and correlated them. We then selected the model with the highest correlation coefficient. Note: a quantitative model comparison (e.g., via bootstrapping or cross-validation) could further rule out competing models, but this is beyond the scope of the current exploratory analysis.

Figure S4A shows the four model predictions simplified by averaging the predicted correlation coefficients across all instances of the same *type* of comparison (e.g., same stimulus type across different sides, different stimulus types within the same side). Those are plotted as bars of four different colors.

Figure S4 B-E shows the measured correlation coefficients for each experiment, simplified in the same manner. The full correlation matrices are shown in **Figure S5.** In each panel of Figure S4B we indicate the model that best matched the measured correlation matrix. For the combined data in Experiments 1 and 2 (for letters and boxes), Model 3 was the best: stimulus-specific factors that generalize across sides. See Figure S4B. The yellow bar is relatively high, due to strong correlations for letters on the right vs. letters on the left, and boxes on the right vs. boxes on the left. According to Williams' t-test (Steiger, 1980), the correlations represented by the yellow bar (same stimulus type, different sides) are significantly higher than those represented by the blue bar (different stimulus, same side) and the red bar (different stimulus, different side). Thus, crowding does not generalize very well across stimulus types, but it does generalize for one stimulus type across locations. See the full correlation matrix again in Figure S2B.

For Experiment 1 (Figure S4C; stimulus types: boxes, emojis, and letters), Model 3 also was the best, although Model 4 was a close second because there is some evidence for a hemifield-specific factor that generalizes partially across stimulus types: the blue bar is elevated compared to the red bar. However, unlike for the combined analysis of Experiment 1 and 2, none of the pairwise comparisons across types of correlations were statistically significant, reflecting the small sample size in Experiment 1 alone (N=15).

For Experiment 2 (Figure S4D; stimulus types: boxes, pseudo-letters, and letters), Model 4 was best, indicating a mixture of both stimulus-specific factors that generalize across sides and side-specific factors that generalize across stimulus types. Interestingly, thresholds for pseudo-letters correlated better with thresholds for boxes than for letters, even though the pseudo-letters were matched to the letters in many visual features (and the number of target alternatives). This suggests that letters suffer less crowding than other stimulus types due to specific mechanisms developed with reading expertise.

However, none of the pairwise comparisons across types of correlations were statistically significant.

For Experiment 3 (Figure S4E; stimulus types: letters flanked either by letters or pseudo-letters), Model 2 was best: side-specific factors that generalize across stimulus types. This is because when correlating thresholds for letter flankers vs. for pseudo-letter flankers, the correlations were stronger within the same side than across sides. Thus, the yellow bar is elevated, as uniquely predicted by Model 2. This suggests that within each visual hemifield, crowding for letters is determined by specific factors that vary across participants but generalize across types of *flankers* (real letters or pseudo-letters). However, none of the pairwise comparisons across types of correlations were statistically significant.

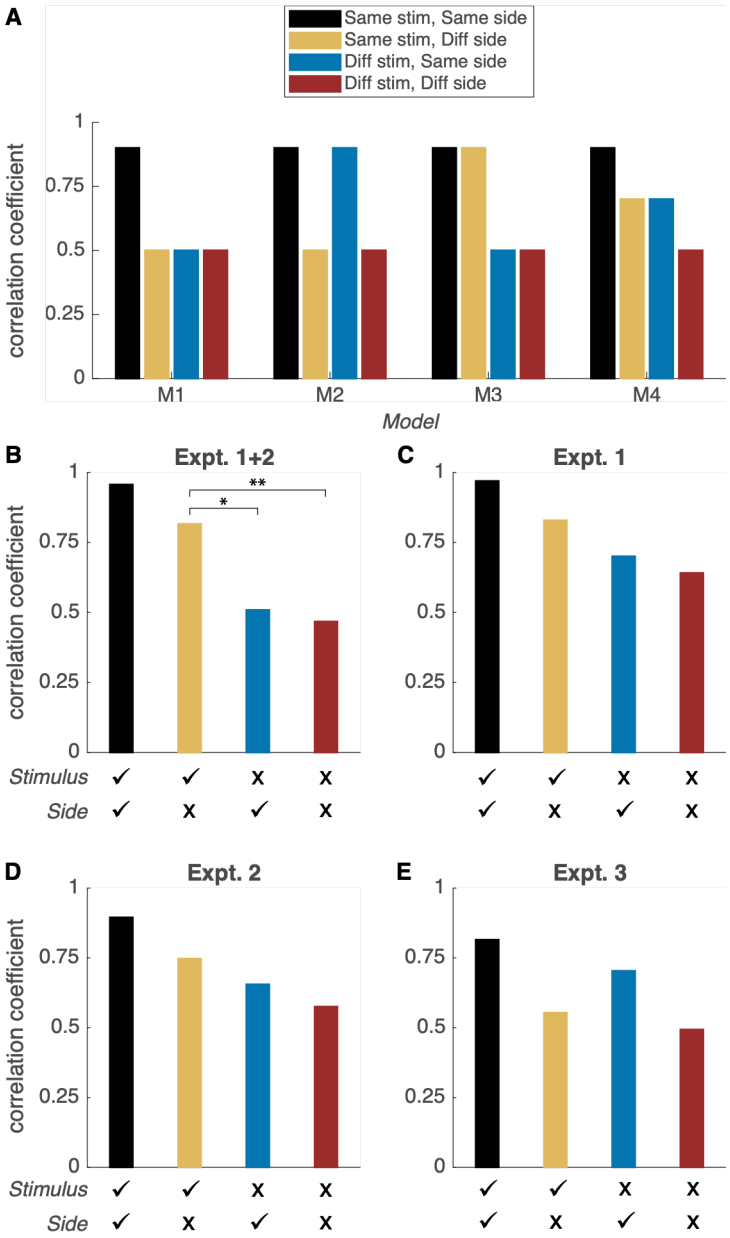

Figure S4: Simplified comparisons across *types* of correlations applied to pairs of conditions with the same or different stimulus types and measured on the same or different sides (i.e., hemifields). These values are generated by averaging across all the values in the full correlation matrices of the same type, as indicated by the color in Figures S3 and S5 (black, gold, blue or red). **(A)** The four models' predicted values for each type of correlation. **(B-E)** Measured correlation coefficients in each experiment. The labels below each x-axis indicate the type of correlation, depending on the match between the stimulus type and side for the two conditions being correlated. A check mark indicates that the two conditions had the same stimulus type or side, and an "x" indicates that the stimulus type or sides were not the same. The asterisks indicate significant pairwise differences between correlation types, according to Williams' t-test (Steiger, 1980).

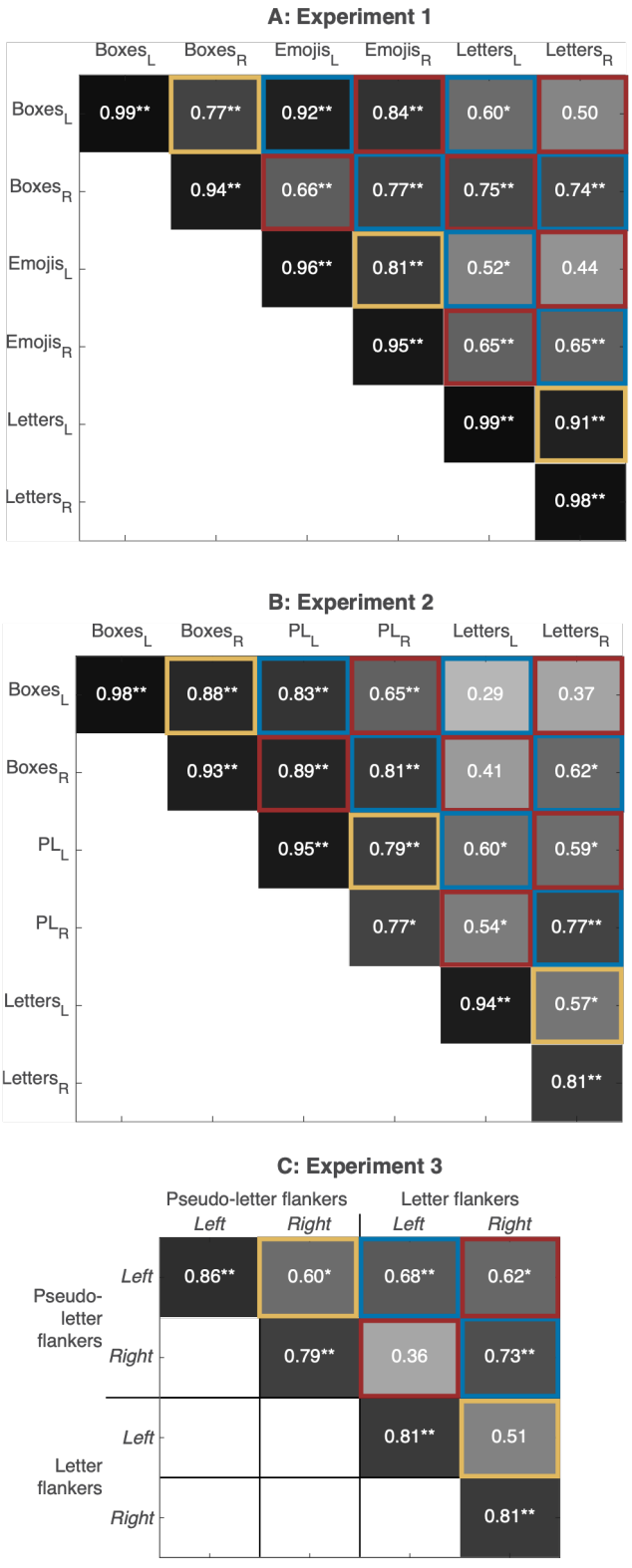

Figure S5: Full correlation matrices for crowding distances in Experiments 1-3. Formatted the same way as Figure S2B. PL = pseudo-letters.

In a final analysis, we examined whether the hemifield asymmetries (expressed as the right:left ratios of crowding distance thresholds) are correlated across stimulus types. The results are plotted as correlation matrices in **Figure S6**.

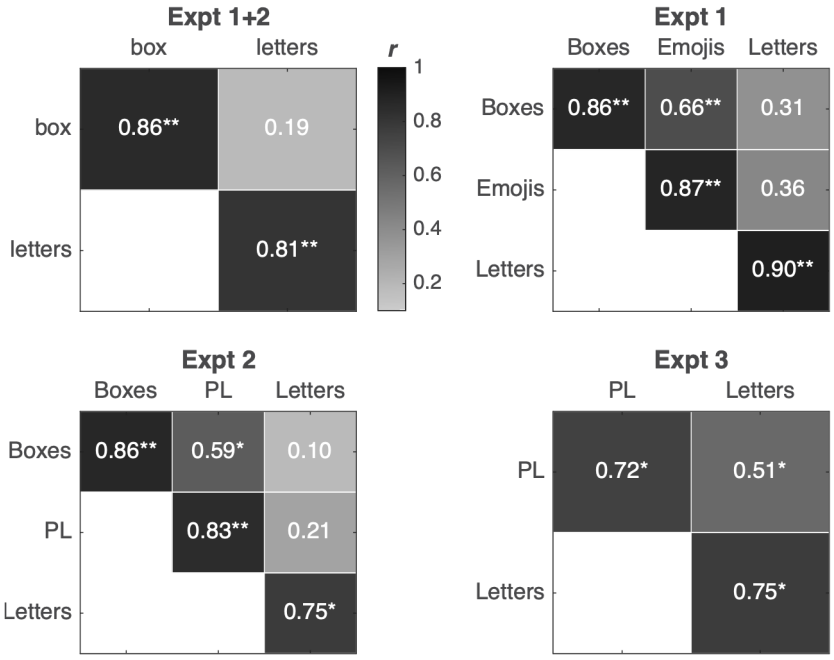

Figure S6: Correlations across individual hemifield asymmetry ratios (right:left) of crowding distances. The values along the diagonal are the split-half reliability estimates, r* (see text). The top left matrix is just for the boxes and letters stimulus types, integrating across the 30 participants in Experiment 1 and 2. The other three matrices are for each individual experiment (N=15 each). Asterisks indicate correlations significantly greater than 0, as in Figure S2B.

The split-half reliabilities (r*) of the hemifield asymmetries within each stimulus type were in the acceptable range (all greater than 0.7). Interestingly, the hemifield asymmetries for boxes correlated moderately well with the asymmetries for emojis (in Experiment 1, r=0.66) and pseudo-letters (in Experiment 2, r=0.59). In Experiment 3, the asymmetry for letters flanked by letters correlated moderately well with the asymmetry for letters flanked by pseudo-letters (r=0.51). But the hemifield asymmetries for letter targets did not correlate well with any other stimulus type (r between 0.1 and 0.36).

This study is underpowered to detect significant differences between these correlations. Even for the comparison of the correlation between boxes and pseudo-letters (r=0.59) vs. the correlation between boxes and letters (r=0.10), the difference is not significant: $t(12)=1.63$, $p=0.13$. A larger follow-up study is needed to confirm that non-letter stimuli correlate better with each other than with letters in terms of hemifield asymmetry.

Nonetheless, these data suggest that the right visual field advantage for letters is generated by a process that has little influence on crowding for other types of stimuli.

The conclusions from these analyses of individual differences are:

(1) Crowding distance thresholds varied widely across individuals, with high test-retest reliability (Kurzawski et al., 2023)

(2) Individual differences partially generalize across visual field locations and stimulus types. We found significant correlations even for pairs of conditions that differ in both the stimulus type and side. These are summarized by the red bars in Figure S4, which hover around r=0.5. These correlations could be due to subject-specific factors that generally influence task performance, such as the degree to which they are attentive and engaged in the task. Such a factor can also be captured by the lapse rate: the probability of making an error even when the stimulus size and spacing are well above threshold. In our analysis, the lapse rate is 1 – the upper asymptote of the psychometric function. Lapse rates differed across stimulus types, being lowest for letter targets. Given the small variation across participants for letters, test-retest reliability was low for lapse rates for letters. But lapse rate reliability was decent for boxes in Experiments 1 and 2 and emojis in Experiment 1 (disattenuated r^* ranging from 0.68 to 0.83). For these conditions, lapse rate correlated significantly with the corresponding distance threshold (r ranging from 0.45 to 0.64). Thus, there is some evidence that subject differences in task engagement account for some correlations in crowding distance thresholds across stimulus type and sides.

(3) Individual variation in crowding thresholds is also stimulus-specific. Crowding thresholds for a particular stimulus at a particular location correlate better with thresholds for the same stimulus type in the opposite hemifield than for a different stimulus type in the same location. This was clear in Experiments 1 and 2, for which the yellow bar in Figure S4B is significantly higher than the blue bar. This is not consistent with a model in which crowding is caused by a very low-level mechanism that integrates features of all stimuli present within certain portions of the visual field. Rather, some individuals have worse crowding for letters than other individuals, which doesn't necessarily mean that they will also have worse crowding for boxes or emojis, or even pseudo-letters with matched visual features. Indeed, crowding for pseudo-letters correlated better with boxes than for letters.

(4) There is also tentative evidence for location-specific crowding mechanisms that vary over individuals. (Kurzawski et al. 2023 stated, "when correlating crowding distances, location matters more than any other stimulus property.") We found that when crossing stimulus types (e.g. letters vs boxes), correlations tended to be higher for the same side than across sides. Compare the blue and red bars in Figure S4. In Experiment 3, when all conditions used letters as the central target but varied in the type of flanker, correlations

were higher for different flanker types on the same side than the same flanker type across sides. Thus, crowding for letters differs in reliable ways across the hemifields. However, none of these pairwise comparisons were statistically significant, and must be followed up with a larger sample size.

(5) The hemifield asymmetries correlate moderately well across various types of stimuli, except for letters. The magnitude of an individual's asymmetry for letters does not well predict their asymmetry for boxes, emojis, or pseudo-letters. Therefore, the right visual field advantage for letters has a unique cause, and it is unlikely that a residual right visual field advantage for other stimulus types is a spill-over effect of expertise with letter recognition.

Altogether, these results support the hypothesis that crowding differs idiosyncratically across individuals and systematically across stimulus types and visual hemifields. We propose that the severity of crowding is influenced not only by general low-level visual factors but also by perceptual learning, that is, shaped by experience and expertise. The reduction of crowding in the right visual field that is specific for letters may further be shaped by the connection between particular shape recognition mechanisms and the language system in the left hemisphere.

References

Barbot, A., Xue, S., & Carrasco, M. (2021). Asymmetries in visual acuity around the visual field. *Journal of Vision*, *21*(1), 1–23. https://doi.org/10.1167/JOV.21.1.2

Benjamini, Y., & Hochberg, Y. (1995). Controlling the False Discovery Rate: A Practical and Powerful Approach to Multiple Testing. *Journal of the Royal Statistical Society. Series B (Methodological)*, *57*(1), 289–300. http://www.jstor.org/stable/10.2307/2346101

Bouma, H., & Legein, C. P. (1977). Foveal and parafoveal recognition of letters and words by dyslexics and by average readers. *Neuropsychologia*, *15*(15), 69–80.

Kurzawski, J. W., Burchell, A., Thapa, D., Winawer, J., Majaj, N. J., & Pelli, D. G. (2023). The Bouma law accounts for crowding in 50 observers. *Journal of Vision*, *23*(8), 1–34. https://doi.org/10.1167/jov.23.8.6

Steiger, J. H. (1980). Tests for comparing elements of a correlation matrix. *Psychological Bulletin*, *87*(2), 245–251. https://doi.org/10.1037/0033-2909.87.2.245